

Quantum computer based on color centers in diamond

Cite as: Appl. Phys. Rev. **8**, 011308 (2021); doi:10.1063/5.0007444

Submitted: 22 May 2020 · Accepted: 28 December 2020 ·

Published Online: 10 February 2021



Sébastien Pezzagna  and Jan Meijer^{a)} 

AFFILIATIONS

Applied Quantum Systems, Felix-Bloch Institute for Solid State Physics, University Leipzig, Linnéstrasse 5, Leipzig, Germany

Note: This paper is part of the Special Topic on Quantum Computing.

^{a)}Author to whom correspondence should be addressed: jan.meijer@uni-leipzig.de

ABSTRACT

Artificial atoms like the nitrogen vacancy (NV) centers in diamond enable the realization of fully functional qubits in a solid at room temperature. The functionalities of all the parts needed to create a quantum computer, such as quantum error correction, couplings, quantum teleportation, and a quantum repeater, have already been experimentally demonstrated. These achievements are expected to influence the industrial development of quantum information technology as well as quantum sensing. Whereas quantum sensing has been established and a large number of organizations are working on new developments in this area, a quantum computer itself remains elusive due to technical reasons and limitations of the available materials. For example, only in recent months has it become possible to electrically readout the NV spin state at the level of a single center and significantly improve the scalability of NV center production. A number of ideas have been proposed to overcome the above-mentioned limitations. This paper summarizes the status of research in the area, details the most promising concepts for development, and discusses factors limiting progress as well as the most recent developments in the field.

© 2021 Author(s). All article content, except where otherwise noted, is licensed under a Creative Commons Attribution (CC BY) license (<http://creativecommons.org/licenses/by/4.0/>). <https://doi.org/10.1063/5.0007444>

TABLE OF CONTENTS

I. INTRODUCTION	1	K. Electron bus system: NV-P1-e-P1-NV	11
II. MAIN PROPERTIES OF SINGLE, COHERENTLY		L. Hybrid concepts: NV-superconducting qubits	11
CONTROLLABLE SPINS IN DIAMOND	2	IV. FROM CLASSICAL QUANTUM INTERFACE TO	
A. Diamond as a host for quantum objects.....	2	QUANTUM DEVICES: READOUT OF QUBITS	11
B. Quantum properties of single-color centers	3	A. Optical spin readout	11
C. Defects and Fermi level adjustment in diamond		B. Electrical spin readout	11
to optimize properties of NV centers	3	V. TECHNICAL REQUIREMENTS AND FABRICATION	
III. BASIC CONCEPTS AND PROPOSALS TO		METHODS FOR SCALABLE DESIGN	12
CONTROL AND ENTANGLE SPIN SYSTEMS	5	A. Diamond in CMOS technology	12
A. Main requirements	5	B. Growth techniques	12
B. Performance	6	C. Deterministic creation of single NV centers with	
C. Error correction	7	high resolution	13
D. Magnetic dipole coupling of electronic NV-NV		D. Thermal treatment	13
and nuclear NV- ¹³ C spins	7	VI. SUMMARIZING PERFORMANCE OF QUBITS	
E. Active decoupling methods of NV or nuclear		BASED ON NV CENTERS	14
qubits from the environment	7	VII. CONCLUSIONS AND OUTLOOK	15
F. Direct NV-N-NV coupling	8	AUTHOR CONTRIBUTIONS	15
G. NV-photon-NV coupling	8		
H. NV- ¹⁵ N-NV- ¹⁵ N by charge state control	9		
I. NV- ¹³ C multi coupling	9		
J. Mechanical control of NV-NV using AFM tips...	10		

I. INTRODUCTION

The discovery of the extraordinary properties of the NV center in 1997¹ raised hopes that a solid-state quantum computer would be

developed soon after.^{2,3} Compared with phosphorous qubits in silicon,⁴ NV centers in a diamond can operate at room temperature. Their creation and control appeared relatively easy,⁵ and their long coherent times offered promise for an easy means of coupling NV centers.^{6–10} The first promising experiments and the possibility of quantum error correction led to hopes that a scalable quantum register with hundreds of qubits could be built within only five to ten years.⁴ Many companies had already attempted to sell single-photon sources based on NV centers, and had shown that quantum information can provide unbreakable and secure data transport.¹¹ On the basis of this technology, schemes to set up a quantum repeater were developed and a quantum Internet was proposed.^{12,13} But 20 years later, the quantum computer remains elusive. After a large investment in research leading to thousands of published papers and dissertations as well as hundreds of patents, it has become clear that the challenge at hand is more daunting than was previously thought. Nevertheless, experiments on a single NV center have yielded a number of exciting results and new sensing applications.^{14,15} In addition to expensive products intended for researchers, the first sensors were developed for the high-value, low-price market, and products for everyday use are now being developed. Moreover, the understanding of ways to couple the electron spin of the NV center with surrounding nuclear spins has led to the development of hyperpolarization schemes that have the potential to revolutionize magnetic resonance imaging (MRI) for medical applications.¹⁶ The research on NV centers has accelerated the transition from nanotechnology to next-generation quantum technology. However, this low-hanging fruit has also motivated many research groups to shift their focus from quantum information to quantum sensing, with only very few concerns still investing time and money in the original goal. Furthermore, owing to past disappointments, the major organizations that fund such research are not willing to spend more money on work on NV centers aimed at building a quantum computer.¹⁷

The development of the quantum information system is comparable to the development of the digital computer. In a digital computer (e.g., CMOS 1.8 V), each measured value of voltage higher than 1.2 V can be interpreted as a “1,” and each value lower than 0.7 V as a “0.” In contrast to the analog computer, exact values are needed in this case.¹⁸ This computer model deals with real numbers, and fault tolerance has to be kept very small. This is the main reason why analog computers are not adequate.

The concept of the quantum computer combines an analog and a digital computer system in a sophisticated way. During quantum computation, the state of the qubit can be represented on the Bloch sphere, and every instance of noise due to the environment has to be considered (like in an analog computer). This means that the quantum processor has to be isolated from the environment. On the contrary, during the measurement procedure, the phase disappears, and only the digital number (e.g., up- or down-spin) is visible. Fortunately, error correction can be carried out to bring the system back into a well-defined state without a measurement procedure. Diamond enables the realization of these concepts at room temperature, and the principles of such an operation in a diamond system at room temperature have already been demonstrated.

In this paper, we review the proposals for and challenges to attaining the goal of a diamond-based quantum computer. Most of the relevant ideas are in their initial stages and are more akin to suggestions than concrete proposals. Their success depends on unknown or

very complex properties of materials, which renders realistic modeling or calculation nearly impossible. A large number of these ideas also lack appropriate methods of fabrication. However, the prospect of building a quantum computer based on a solid-state system is important and a review of work in the area is thus justified.

II. MAIN PROPERTIES OF SINGLE, COHERENTLY CONTROLLABLE SPINS IN DIAMOND

A. Diamond as a host for quantum objects

Building a quantum computer optimally involves isolating a system from the environment while ensuring the greatest possible control over it.¹⁹ Both requirements are impossible to fulfill according to quantum mechanical laws. The solution lies in a compromise such that the best possible separation from the environment can be achieved together with individual qubit control. The optimal conditions for this are found in vacuum. In this way, any disturbance can be shielded, and the qubits can be controlled by means of electromagnetic waves. It is therefore not surprising that ion traps at present have achieved the best results, setting a record in terms of the possibility of controlling qubits.^{20,21} The disadvantage of this method is that the qubits have to be placed in spatial coordinates to control their position. When using ion traps, this is possible only with a large amount of effort. The vacuum must also be very good (better than 10^{-12} mbar), which implies stringent technical constraints. Such systems are therefore unsuitable for everyday use, and their scalability is technically complex. Much better scalability can be achieved with a superconducting qubit scheme, as shown recently by Google.²² However, superconducting qubits are large and work only at a very low temperature. This also limits their scalability to a few hundred.

A solid-state solution is therefore desirable and can be connected more easily with current CMOS technology.²³ Quantum objects are automatically fixed in the solid, and the qubits maintain their position even in the case of the failure of technical devices. The defect-free isotopic ¹²C diamond crystal, with its large bandgap of 5.4 eV, has properties similar to those of a vacuum; thus, a point defect center can be compared to an atom in a trap.^{10,24}

The large bandgap ensures that even at room temperature, the conduction band remains unoccupied and no free electrons can unintentionally interact with the qubits. The strong covalent bonds provide a high Debye temperature of over 1800 K so that few phonons disturb the system.²⁵ The low diffusion constants of almost all elements enable the atoms to retain their positions even at temperatures of several hundred Kelvin.

Because of the well-defined properties of defects based on single atoms, all quantum devices have similar electronic structures, spectral lines, and spin properties. This is their main advantage over solid-state quantum devices based on quantum dots, for which the number of atoms and structure differ. However, this is the ideal case that is valid only inside the bulk of a diamond. In practice, the crystal is imperfect, and magnetic atoms such as ¹³C, which has a nuclear spin, or impurity atoms like nitrogen, which has an electron spin, disturb the quantum phase.

To manipulate and read out a specific qubit, an interaction with a classical medium is used such that this can be carried out in two ways. The first is as a gate operation in which the state is changed in a defined way but not read out. The quantum system remains a self-contained isolated system. The second way involves actual measurement where the quantum state is read out. This is also connected to a

change of state in the sense of quantum mechanical rules. Here, a connection with the classical world takes place, and the system can no longer be regarded as isolated. If possible, the measurement can be made as a so-called “single-shot readout.”²⁶ This is not a single measurement, but further measurements should not change the result. For example, it is possible to read out a nuclear spin using an NV center several times without changing the state of the nuclear spin.²⁶

Only two defect centers in diamond exhibit properties that make controlling their spin states at room temperature possible: the NV and the ST1 centers.^{27,28} At low temperature, the spin state of SiV centers can be coherently controlled as well, but their T_2 times are very short.²⁹ With regard to the state of the art, the NV center remains the main candidate for coherently controlling single spin. It is composed of a nitrogen atom with a nuclear spin of 1 (^{14}N) or $1/2$ (^{15}N) and a first-neighbor carbon vacancy. In the negatively charged state of the NV, the electrons build a triplet state with a zero-field splitting of 2.87 GHz.³⁰ The main advantage is that the $m=0$ spin state exhibits different behavior during optical cycles than the $m=\pm 1$ spin state. Thus, an initialization as well as a readout of the spin state is possible. In a two-qubit scheme, the $m=0$ state can be defined as a $|0\rangle$ state and $m=-1$ as a $|1\rangle$ qubit state.

Figure 1 shows the scheme of the energy levels of the NV⁻ center. The center has been well described in the literature.^{17,30,31} Compared with quantum dots, the NV center is a kind of artificial atom with similar, well-reproducible properties that can be created via ion implantation or during diamond growth.

B. Quantum properties of single-color centers

The quantum properties are defined by the Hamiltonian of the NV center,³⁰

$$\mathcal{H} = D S_z + \gamma_S \vec{S} \cdot \vec{B} + \vec{S} \cdot \vec{A} \cdot \vec{B} + \gamma_I \vec{I} \cdot \vec{B}. \quad (1)$$

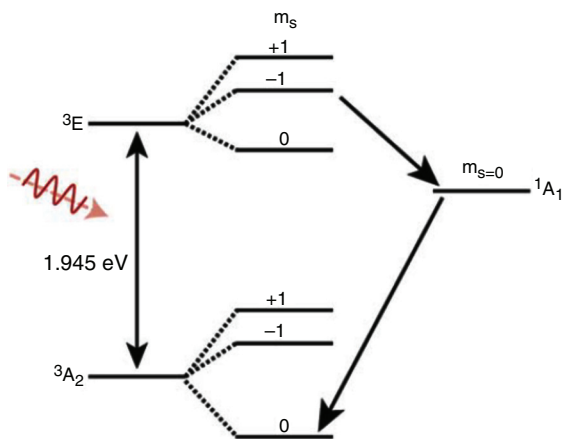


FIG. 1. Energy level scheme of the NV center. The ground and excited states are triplet states. There is a 30% mixing by the interband coupling of $m=\pm 1$ with the singlet state and the $m=0$ in the ground state. This behavior leads to an easy and efficient polarization of the spin state to $m=0$ by optical pumping [Weber *et al.*, “Quantum computing with defects,” Proceedings of the National Academy of Sciences of the United States of America **107**(19), 8513–8518 (2010), licensed under a Creative Commons Attribution (CC BY) license].⁴

Typically, charged color centers possess a singlet ground state and are transformed into a triplet by excitation.³² An example is the ST1 (or L2 center).^{27,33} Spin polarization is obtained when a state of the triplet is preferentially occupied. For the NV center, the situation is the opposite. In the ground state, it is in a triplet state, and the singlet is reached via intersystem crossing from the excited state (Fig. 1). The spin polarization then takes place exactly via the singlet state toward which the transition rates for $m=1$ and $m=-1$ are significantly stronger than for $m=0$.^{34,35} Because the singlet decays back into the triplet states with similar transition rates, the spin polarization likely occurs due only to the first decay from the excited triplet to the singlet.³⁶ Therefore, after only a few excitation cycles, a spin polarization with a probability of 98% is achieved. As is shown in Eq. (1), even when no external magnetic field is applied, the ground state is also split by a spin orbital interaction with an energy of 2.87 GHz $\times h$. The polarization of the ground state is also given by the spin orbital interaction. The spin state can be controlled by applying microwave pulses. The NV center is characterized by a long coherence time because phonon interaction is suppressed. In an isotopically pure diamond, coherence times (T_2) of several milliseconds are achievable at room temperature. Figure 2 shows Rabi oscillations driven on a single NV center. A π -pulse leads to a conversion of the state $m=0$ (e.g., qubit $|0\rangle$ state) to $m=-1$ (e.g., qubit $|1\rangle$) and can be realized in ~ 7 ns.^{37,38} Other centers, like the SiV or ST1, do not exhibit such a long coherence time.²⁷

The properties of the NV can be improved by antenna structures or even a Förster transfer.³⁹ However, it is not possible at present to electrically excite and initialize NVs. This is an obstacle to the production of sensors and limits the design of NV-based quantum computers. Thus, only all NV centers can be initialized in a register at the same time. While initialization is performed by using a laser pulse, gate operations are achieved by microwave pulses. The simplest variant involves determining the Rabi frequency (Fig. 2) and defining different gate operations via the microwave pulse length in combination with the defined waiting times.⁴⁰ Two-gate operations are extended in a similar way, where a conditional gate operation is achieved via a small bandwidth of the microwave pulses depending on the state of the second qubit. These operations are also performed in combination with the defined waiting times.^{41,42} The times at which the gate operations can be performed depend on the intensity of the microwaves, the coupling with the NV, and the interference due to the bandwidth. Typical gate times for a π -pulse are approximately 10 ns.^{43,44} With a coherence time of a few milliseconds, 10^4 gate operations can be carried out. Although the number of operations appears to be large, many gate operations are required, e.g., for error correction or for SWAP gates on the nuclear spin (see Sec. III). The number of gate operations can be improved by extending the T_2 times, actively decoupling the environment and parallelizing the gate operations. The corresponding concepts are presented in Sec. III. Figure 3 shows the detected magnetic resonance spectra of an NV center with hyperfine coupling to ^{14}N in the ground state. This coupling allows researchers to swap an electron’s spin state with the nuclear spin state to prolong coherence times.

C. Defects and Fermi level adjustment in diamond to optimize properties of NV centers

To use the color centers as qubits, it is necessary to control their crystal environment. The quality of the crystal structure, and the presence of foreign atoms or defects with unsaturated electron spins and

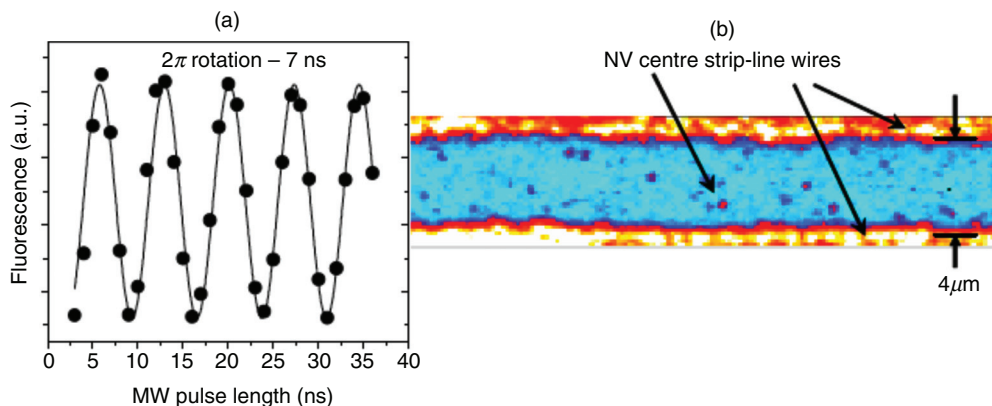


FIG. 2. (a) Rabi oscillation of a single NV center. (b) Confocal fluorescence image of a sample showing microwave strip line wires and scarce NV centers. Reproduced with permission from J. Wrachtrup and F. Jelezko, “Processing quantum information in diamond,” *J. Phys.-Condens. Matter* **18**(21), S807–S824 (2006).³²

nuclear spins has to be considered. The quality of the surrounding crystal structure is determined by simple point defects, extended defects, or impurity atoms. The defects lead to stress and unwanted electrical properties, such as a local shift of the Fermi level as well as unsaturated electron and nuclear spins. The electron spins are particularly critical for color centers because their range of interaction is of the order of several nanometers and strongly influences the coherence times. The defects can also be ionized by a laser pulse that can promote free electrons in the conduction band. These free Bloch electrons have a very long range (up to several μm). Point defects can be annealed relatively easily by means of a temperature treatment. Extended defects are typically more stable and cannot be easily destroyed. In the case of implanted NV centers, the main challenge is to remove isolated vacancies (which mainly act as electron traps and perturb the negative charge state stability of the NV) and di-vacancies (paramagnetic defects that reduce NV coherence) or larger vacancy complexes. V^0 and V_2^0 start to anneal at 600°C and 850°C , respectively, and an

optimal T_2 is obtained for annealing at 1100°C .⁴⁵ However, the kinetics of the defects and impurities during thermal annealing may be strongly modified if they possess different charge states. This has been the focus of recent work: considering the charging of vacancies (either to V^+ or V^-) by diamond doping (p-type⁴⁶ or n-type doping⁴⁷) to reduce V_2 and larger complexes formed by Coulomb repulsion. This led to a more stable NV^- charge state and an improvement in T_2 . The NV creation yield was enhanced by one order of magnitude and was up to 75%. Furthermore, the role of hydrogen in the passivation of NV through the formation of NVH was also shown to be strongly dependent on diamond doping. Note that the band-bending close to the surface of diamond likely modifies the kinetics of defect formation with respect to those of bulk diamond.

While the p-type doping of acceptors in diamond by boron ion implantation has been carried out for a while and yielded good results,⁴⁸ the doping of donors by phosphor, nitrogen, or sulfur ion implantation is considered impossible.⁴⁹ However, the relevant studies

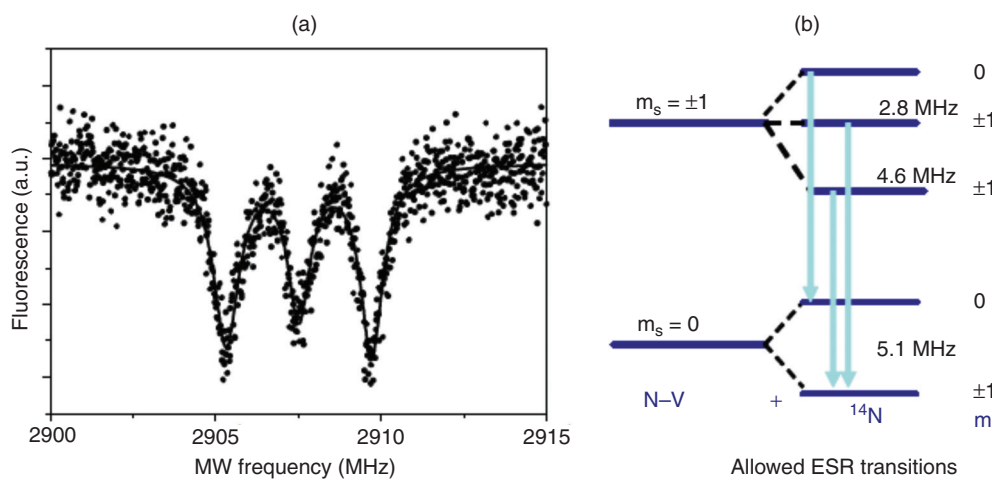


FIG. 3. (a) Optically detected magnetic resonance spectrum from a single NV color center. (b) Energy level scheme for the NV center showing hyperfine coupling in the ground state spin substructure. Reproduced with permission from J. Wrachtrup and F. Jelezko, “Processing quantum information in diamond,” *J. Phys.-Condens. Matter* **18**(21), S807–S824 (2006).³²

have been based on measurements of the Hall effect, and whether the doping failed overall or the electrons were captured only by the defects generated during the implantation was not determined. Even if n-type conductivity was not obtained, this is not important here because it is precisely the capture of electrons that needs to be exploited to charge the vacancies. A simple method to determine the charge state of isolated vacancies is through optical spectroscopy.¹⁷ The PL emission line at 741 nm corresponds to the neutral charge state V^0 , whereas negatively charged vacancies V^- (ND1) exhibit absorption in the ultraviolet band, and V^+ is not known to be optically active. PL spectra have been used to prove vacancy charging when carbon was implanted into an n-type-like diamond previously doped with phosphorous donors. As a consequence, the formation and properties of the NVs significantly improved, not only through phosphorous doping but also through doping by oxygen and sulfur. Further investigation (both theoretical and experimental) is needed, however, on the choice of the best donor atom for the given coherence time of the NV. In addition to charge, the presence of hydrogen is an important parameter. Hydrogen is a mobile species in diamond at relatively high temperatures and can bind to an NV center to form NVH.^{50–52}

Typical values for the diffusion coefficient of hydrogen are $0.06 \text{ nm}^2/\text{s}$ at 550°C and $1000 \text{ nm}^2/\text{s}$ at 850°C (activation energy of about 2.5 eV), but are strongly dependent on its charge state.^{17,53} NVH is optically inactive, and the NV center can no longer be used as a qubit. To prevent this capture, either a diamond with the lowest possible H content must be used, or hydrogen must be prevented from diffusing or forced to bind to another defect. The high conversion rate of the implanted N into NV in donor-doped diamond likely takes advantage of such an effect, together with the larger availability of isolated vacancies enabled by Coulomb repulsion. Note that the same passivation-related issues as for NVs occur also for dopants with the formation of BH or PH.⁵⁴

Only negatively charged NV^- centers allow for a simple and coherent control of the spin. It is therefore necessary to pin the local Fermi level above the $NV^{(0/-)}$ transition level using the presence of donors. The NV centers are charged by a tunnel effect.⁵⁵ It has also been shown that the donor atom “giving” its electron to the NV can be the same over several months.⁵⁶

By applying voltage, the charge of NV centers can be controlled. That this is possible from NV^- to NV^0 has been shown by many research groups and has also been observed in bulk.^{57,58} The switching from NV^0 to NV^+ was achieved only for near-surface NVs. In this case, the surface of the diamond was terminated with hydrogen, which produced significant band bending on the surface.⁵⁹ Figure 4(e) shows the band deflection and the principle of switching the charge of an NV center. The dark state represents NV^+ . The switching of the charge state in the NV^+ state has no electron spin, which allows for switching off the qubit. This in turns allows for the design of a quantum computer according to the concept described in Sec. III.

III. BASIC CONCEPTS AND PROPOSALS TO CONTROL AND ENTANGLE SPIN SYSTEMS

A. Main requirements

All prerequisites for producing a fully functional quantum computer (QC) based on NV centers have been met. What would such a chip look like? The essential features of a quantum system for building a quantum computer were initially summarized in the DiVincenzo

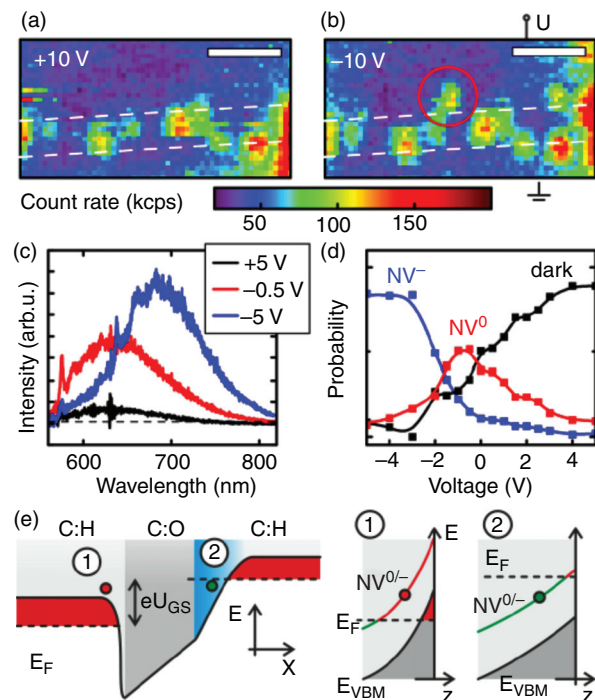


FIG. 4. Applied voltage of p-n-p junction fabricated by oxygen, hydrogen, and oxygen surface termination. (a) The NV^+ center at an applied voltage of $+10 \text{ V}$. (b) NV^- obtained using an applied voltage of -10 V . (c) Spectra of the NV centers at different voltages. (d) Charge state of the NV center at different voltages. (e) Level scheme for different surface terminations. Reproduced with permission from M. V. Hauf *et al.*, “Addressing single nitrogen-vacancy centers in diamond with transparent in-plane gate structures,” *Nano Lett.* **14**(5), 2359–2364 (2014).⁶⁰

conditions.^{61–63} NVs have well-defined properties as color centers in diamond and are well understood.²⁵ In the past few months, breakthroughs have been made in the scalability of an NV-based system in terms of both the deterministic implantation of countable single ions at a high resolution⁶⁴ (see Sec. V) and the efficient conversion of implanted nitrogen atoms into NV centers⁴⁷ (see Sec. II C), and this has been improved further in terms of optical and spin properties. NVs can currently be generated with a probability of up to 75% by using charge-assisted defect engineering. The initialization stage of qubits is easy to fulfill, as was shown in 2001.^{2,65,66} This is, however, not possible electronically but only by means of a light pulse. As shown in Fig. 1, the $m = \pm 1$ state has a 30% chance of undergoing a non-radiative intersystem crossing to the singlet state and decaying to the $m = 0$ state, whereas the state $m = 0$ does not couple to the singlet. This means that after about 10 cycles, the NV center is polarized to 98% at room temperature. This is of course not sufficient for a quantum computer to achieve a meaningful fidelity of 99.99%. One can change to low temperatures or to a ^{13}C transferring spin state procedure.

A disadvantage of the optical readout occurs because of a tenfold hyperfine interaction that is stronger in the excited state than in the ground state. This disturbs both the surrounding NV and the nuclear spin states. A partial readout is therefore currently not possible for many applications, but is also not necessary. This leads to a reduction

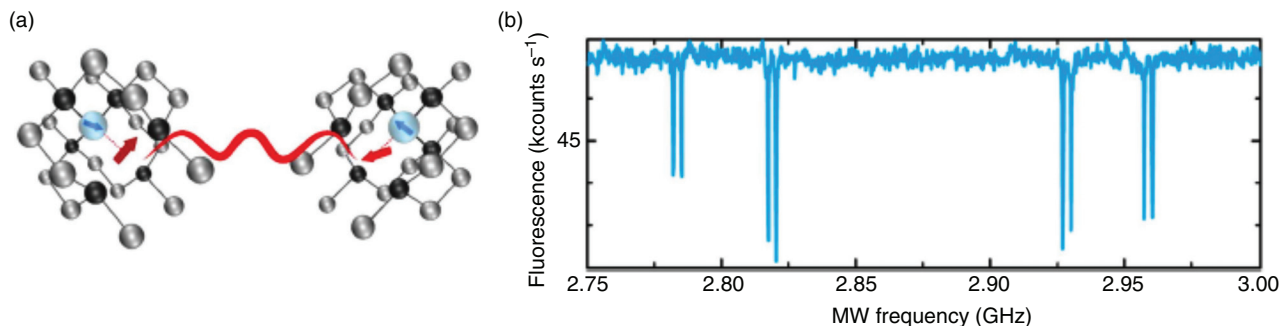


FIG. 5. (a) Interaction of the electron spins of two NV centers. (b) Optically detected magnetic resonance ODMR spectra of two coupled NV centers. The outer pairs of transitions correspond to NV1 and the inner pairs to NV2. The splitting of 3 MHz within a pair occurs owing to hyperfine coupling with the ¹⁵N nucleus. Spin transitions of distant NV centers are separated by 30 MHz. Reproduced with permission from F. Dolde *et al.*, “High-fidelity spin entanglement using optimal control,” Nat. Communications **5**, 3371 (2014).⁴¹

in the coherence time because, in addition to the NV, defect centers are activated and free spin states develop. An improvement by means of electrical excitation would be advantageous. A first attempt in this direction has recently been successful with a Forster excitation.³⁹ To achieve a universal set of gates, it is necessary to realize a NOT gate as a single-qubit gate operation and a controlled-NOT (CNOT) as a two-qubit universal gate.² A coherent spin state switching of the NV can easily be realized by a microwave pulse of a certain length and intensity, the so-called π -pulse. This π -pulse represents the NOT gate. The resonant frequency is defined by the spin state of nearby centers or nuclear spins, because of which a narrow-band microwave π -pulse allows for the realization of a controlled rotation (CROT) or, in combination with an additional rotation, a CNOT gate. The CROT gate is, for NV centers, equivalent to the CNOT gate. Only if the controlled qubit is in the $|1\rangle$ state is the target gate resonant with the microwave field and the target qubit flips. Of course, the gate requires a linewidth that is small enough. Figure 5(a) shows the scheme of an interaction between NV centers with different orientations by means of magnetic dipole-dipole interaction. The different orientations lead to different splittings of the magnetic resonances as detected by optically detected magnetic resonance (ODMR) [Fig. 5(b)]. Thus, each NV can be manipulated individually. The magnetic dipole field interaction is related to the quantum state m . A control qubit can only be flipped if the target qubit is in the correct state; otherwise, the microwave frequency for the π -pulse does not match the transmission frequency.

The single-shot procedure has been carried out using nuclear spins.^{26,67} In this method, the spin state of the NV center is exchanged with the state of the nucleus. The spin state can be transferred by a SWAP gate process. The SWAP process can be achieved, e.g., by three CNOT gate operations. Figure 6 shows a scheme of qubit teleportation. In this case, the nuclear singlet spin is transformed into a triplet state $|+\rangle$ or $|-\rangle$ using double quantum transitions, which requires the use of five CNOT gates. This enables the reading of the spin state several thousand times without changing the nuclear spin state. This is the only way to successfully perform an optical or an electrical readout.

The best coherence times are currently possible in slightly n-type-doped ¹³C free diamonds,^{10,68,69} and can reach 2 ms at room temperature. Using nuclear spins, this time can be extended to the order of seconds.⁷⁰ Assuming a process time of the gate operation of 10 ns,

several 10^7 gate operations can be performed, including nuclear spin. However, error correction requires several 1000 gate operations. Possible “flying qubits” are realizable by photons,⁷¹ phonons,⁷² or electrons.^{73,74} None of the previously proposed methods can ensure reliable operation. An alternative is to use a small number of qubit NVs as a register and build a chain of NVs. The transfer operations, however, strongly limit the number of qubits. The realization of flying qubits is one of the biggest hurdles to building a fully functioning quantum computer with more than 1000 qubits.

B. Performance

The qubit systems realized in diamond or SiC are characterized by excellent quantum control, and single qubit gates with a fidelity of 99.99% and double qubit gates with that of 99.2% have already been demonstrated.⁷⁵ Entanglement and high-quality quantum algorithms in chips with up to 10 quantum bits have also been demonstrated, with coherent control for up to 30 spins⁷⁶ (see Sec. III I). Thus, solid-state spin systems are already comparable to superconducting quantum bits and better than competing systems, as shown in Table I.

Spins of dopants in diamond or SiC are among the most controllable quantum bits in solids.⁷⁷ They can be manufactured deterministically within a spatial accuracy of a few nanometers.⁶⁴ Electron or nuclear spins are available as qubits. Their coherence times are in the range of a few seconds depending on the type of qubit.⁷⁵ One- and two-qubit gate operations with a precision of 99.95% have been demonstrated.⁴¹ The initialization or readouts of qubits with qualities

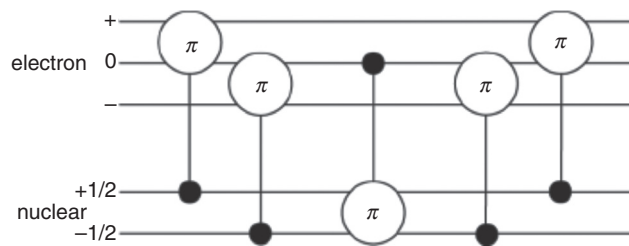


FIG. 6. Swap scheme to transfer the spin state from electron spin to nuclear spin. Reproduced with permission from F. Dolde *et al.*, “High-fidelity spin entanglement using optimal control,” Nat. Communications **5**, 3371 (2014).⁴¹

TABLE I. Comparison of benchmarks for different solid-state systems.

Qubit (host)	T ₂ [ms]	Benchmarking one-qubit gate	Gate error two-qubit gate	Ref.
NV (diamond)	60 000	99.995%	99.2%	70,78
P (Si)	30 000	99.9%	—	82,83
Superconducting	0.1	99.92%	99.4%	84,85
e ⁻ (GaAs)	0.001	98%	90%	86
e ⁻ (Si)	0.1	99.9%	94.7%	87

higher than 95% have also been demonstrated,²⁶ and the entanglement of several electron quantum bits, or “entanglement swapping” on adjacent quantum bits, has been proven.⁴² NV centers are one of a few quantum systems that allow a repetitive error correction.⁷⁸ Other quantum algorithms, such as the quantum Fourier transformation or algorithms for the simulation of simple molecular compounds, have been proposed⁷⁹ and have yielded pulse sequences for quantum gates with qualities above the fault tolerance threshold.⁸⁰ The strong coupling of defects is the essential basis for scalability.⁸¹

C. Error correction

To operate a quantum computer, error correction is necessary.^{88,89} Different error correction methods have been developed and can all be applied to NV qubits. The simplest methods are based on five or seven qubits,⁹⁰ and complex ones are based on up to 100 qubits. The choice of error correction protocol depends on the quality of the qubits. With a fidelity of >99.99%, only a few qubits are sufficient. If the fidelity drops, a large number of qubits is needed to achieve sufficient correction.⁹¹ The main task is therefore to achieve a fidelity as high as possible. For the NV, an average gate fidelity of a single qubit has been measured to be 0.999 952(6), and that of a two-qubit-CNOT gate reaches 0.992(1) at room temperature. NV centers are one of the few systems where the concept of error correction has been successfully demonstrated. Three-qubit systems were tested at room temperature⁹¹ and exhibited a very high fidelity at 4 K.⁹²

D. Magnetic dipole coupling of electronic NV–NV and nuclear NV–¹³C spins

To couple qubits, an interaction must exist or have existed. For NV spin systems, the coupling is achieved by magnetic dipole–dipole interaction. The field strengths of single spins are extremely high in the near field. Magnetic field strengths of 1 T can be achieved at a distance of 2 nm. The dipole–dipole interaction is given by

$$\mathcal{H}_{\text{dip}} = \frac{\mu_0 \gamma_e^2}{4\pi r_{AB}^3} [S_A S_B - 3(S_A + n_{AB})(n_{AB} S_B)]. \quad (2)$$

Because the dipole–dipole interaction is dependent on r⁻³, the lateral resolution in which an optimal structure of a quantum computer needs to be achieved is very strongly limited. The NV–NV coupling has an energy of $\hbar \times 10$ kHz for a 30 nm separation. For the NV–¹³C coupling (hyperfine interaction), this is about $\hbar \times 12$ MHz if the ¹³C is located within the first shell. The couplings of it with ¹⁴N and ¹⁵N can

be carried out at 2 and 5 MHz, respectively, in the ground state. A too weak coupling strength leads to long switching times for two-qubit gates, such as a CNOT, while a too high coupling strength reduces the coherence times of the qubits.⁵⁵ Relaxation times due to spin flip-flop depend on r⁻⁶. A trade-off therefore needs to be found between these extremes. An optimal value for the NV–NV coupling is likely reached at a distance of 10 to 20 nm. This corresponds to a coupling strength of a few MHz and can be used to realize short switching times. This is the only way to achieve a sufficient number of switching times within the coherence time. A disadvantage of solid-state systems is that the coupling strength cannot be adjusted and is determined only by the distance between the NVs. By clever selection of the spins, like double quantum transition (DQT), the value can be quadrupled with the disadvantage, however, that the coherence time is halved.⁹³ However, as discussed in Sec. III E, one can extend the coherence times T₂* to T₂, for example, from a value of T₂* of 22 μs to that of T₂ of 500 μs,⁹⁴ by dressing modes and refocusing procedures. Another possibility is the inclusion of nuclear spins (Fig. 7). Nuclear spins have a magnetic field three orders of magnitude lower, and the coupling is correspondingly smaller. However, this lower coupling also leads to a greater decoupling to the environment, which results in a long coherence time. The T₂ times can reach up to seconds at room temperature. Nuclear spins are therefore ideal quantum memories.⁹¹ Figure 7 illustrates this kind of coupling between one NV and three nuclear spins.

E. Active decoupling methods of NV or nuclear qubits from the environment

The importance of the coherence time T₂ has already been noted several times. The QC can be used only within T₂. The width of the lines and, thus, the design of the CNOT gates also depends on the coherence time. The coherence time is limited by disturbances, which in most cases are owing to unsaturated spin systems such as ¹³C nuclear spins, but can also be caused by disturbances outside the sample. Because the coupling to the spin system is mainly affected by the magnetic components of the electromagnetic field, only disturbances caused by magnetic fields are to be considered. These magnetic disturbances from outside can have certain defined frequencies but also a wide noise spectrum, accordingly.⁹⁵ In the first case, refocusing is possible using known pulse sequences, such as the XY8 pulse sequence. The limited coherence time caused by noise only is called T₂, and the limited coherence time caused by defined disturbances is called T₂*. T₂* is therefore always shorter than T₂. To prevent interference from direct spin couplings, such as ¹³C nuclear spins, double frequency excitations are possible. This method is also called spin state dressing and allows for the decoupling of nuclear spins from the NV center,⁹ but can also be used to prevent electron spin crossover during gate operations of nuclear spin.⁷⁰ In the latter case, a CROT gate has been built to achieve the coupling of an NV with nine nuclear spins.⁷⁵ Another possibility is to polarize the spin bath to achieve a defined constant magnetic field. The polarization of the spin bath is also called hyperpolarization, where this method is known in the nuclear magnetic resonance (NMR) technique.⁹⁶ The spin of an NV center is used to polarize the surrounding dark spins. To achieve polarization, an optimal coupling from the NV center to the nuclear spins is necessary for a certain time. This is achieved by a Hartmann–Hahn condition, or by means of the P1 centers (substitutional neutral nitrogen atoms).⁹⁷

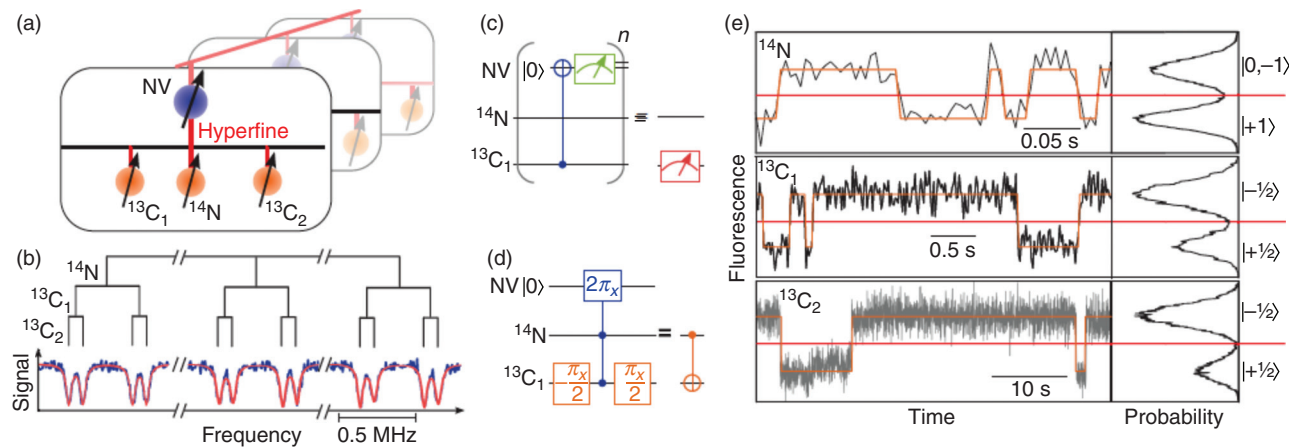


FIG. 7. (a) Illustration of the quantum register consisting of three nuclear spins (orange circles with black arrows) coupled by hyperfine interaction to the NV electron spin (blue circles with black arrows), forming a prototype single node of a larger register. ¹³C_{1,2} refers to ¹³C nuclei at different lattice positions. (b) Hyperfine splitting (¹⁴N, 2.16 MHz; ¹³C₁, 413 kHz; ¹³C₂, 89 kHz) of the transition of $m_S = 0$ to -1 into 12 individual lines. (c) Wire diagram of the projective readout of nuclear spins; the diagram here is that of a ¹³C spin. (d) Wire diagram of a CNOT gate between two nuclear spins. (e) Left side: time trace of NV fluorescence photons during repetitive readout of a particular nuclear spin [see (c)]. The timescales of the dynamics depend on the lifetimes of the nuclear spins and durations of the CNOT gate. Right side: photon-counting histograms of the time traces. The red line indicates the threshold for nuclear spin state discrimination. Reproduced with permission from G. Waldherr *et al.*, “Quantum error correction in a solid-state hybrid spin register,” *Nature* **506**(7487), 204 (2014).⁹¹

F. Direct NV-N-NV coupling

In addition to the direct NV–NV coupling, electronic dark spins can be included, just like nuclear spins. The coupling is NV–N–NV,⁵⁵ or even the spin chain NV–N–N–N... N–NV.⁹⁷ One method involves energy transitions in the overlap between the NV center and the P1 center, due to the Zeeman effect, at a magnetic field of 51.2 mT. Figure 8 shows the distributions of the N and NV centers created by implantation. Figure 8(c) shows the possible level transitions between NV and N. This allows for a resonant coupling between the electron spins of NV and P1 in order to undergo a targeted spin exchange.⁹⁸

This spin exchange can then be extended to several P1s via dipole–dipole coupling, as shown in Fig. 9. However, simulations show that decoherence is a problem for longer spin chains, and these chains are not controllable. This hardening has applications both in hyperpolarization and methods of electrical readout (see Sec. IV).

G. NV-photon–NV coupling

In this concept, the NV is coupled directly with photons to achieve the transfer of spin via the photon. The advantage is that a real

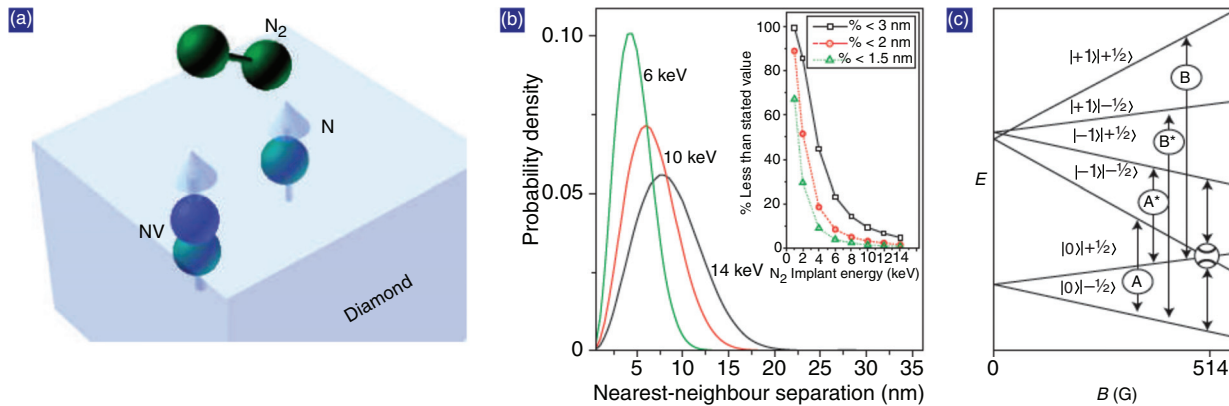


FIG. 8. (a) Schematic diagram of molecular implantation leading to the formation of NV–N spin pairs. After entering the diamond, the chemical bond of the N_2^+ molecule is broken, and the two N atoms penetrate independently into the diamond. Hence, the implantation of single N_2^+ ions leads to the formation of N–N pairs and vacancies (V) in the diamond substrate. Annealing leads to the conversion of some of the N into NV, leading to closely spaced NV–N pairs. (b) Monte Carlo simulation of the distribution of intrapair spacings for implantations of 14-, 10-, and 6-keV N_2^+ dimers. The inset shows the calculated fraction of the implanted pairs, with separations between the N defects smaller than 3, 2, and 1.5 nm as a function of N_2 implantation energy. (c) Energy levels of a dipole–dipole-coupled NV–N pair. The separation between the N states in the excited NV manifold at low *B* is the dipolar coupling, $\Delta = 13$ MHz. Reproduced with permission from T. Gaebel *et al.*, “Room-temperature coherent coupling of single spins in diamond,” *Nat. Phys.* **2**(6), 408–413 (2006).⁹⁸

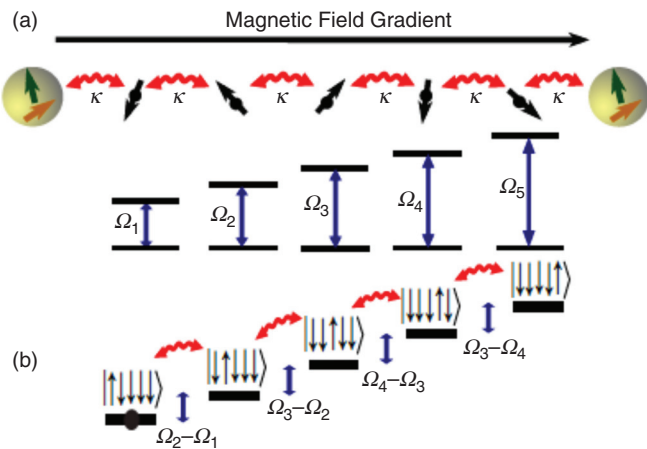


FIG. 9. (a) Each NV register contains a nuclear spin $I = 1/2$ (yellow), providing quantum memory, and an electronic spin $S = 1$ (green). Dark spins (black) represent elements of an optically unaddressable spin chain, which coherently couples spatially separated NV registers. The NV level structure (in a high B field) is shown. A resonant pulse coherently transfers the electronic spin of the register from 0 e to 1 e. Subsequent manipulation of the nuclear spin is accomplished through a radio-frequency (RF) pulse. The far detuned state can be neglected to create an effective two-qubit register. However, the full three-level NV structure is utilized by the coherent coupling of the NV registers. Reproduced with permission from N. Y. Yao *et al.*, “Scalable architecture for a room temperature solid-state quantum information processor,” *Nat. Communications* **3**, 800 (2012).⁹⁷

flying qubit is thus obtained. Due to the linewidths, this method can be used only at very low temperatures, and the coupling with the photon field must be very strong. This can be achieved by means of a cavity. Another major advantage is that long stretches can be overcome, and the construction of a quantum network becomes conceivable. Figure 10 shows an example of a waveguide based on silica on silicon with a 50:50 beam splitter. This waveguide can be used to couple a resonator with a single NV center.

H. NV-¹⁵N-NV-¹⁵N by charge state control

In this concept, the charge state of the NV centers is used to switch the NVs. For the NVs, three charge states are known: NV⁻, NV⁰, and NV⁺. While NV⁻ has the well-known triplet, NV⁰ is a singlet state, and NV⁺ has no luminescence and should have no spin, similar to ¹²C (i.e., it is diamond metric). By switching from NV⁻ to NV⁺, the coupling to ¹³C nuclei as well as to adjacent NVs can be switched on and off. This allows researchers to address NV centers and read out single NVs (because the information is transferred to the neighboring ¹³C). Figures 11 and 12 show the structure and functionality of this idea.

I. NV-¹³C multi coupling

Recently, 27 nuclear spins were coupled to an NV center and switched separately by using the fact that, at low temperatures, the linewidths narrow and the coherence time of the nuclear spins increases.⁷⁶ The hyperfine interaction involves permanently coupling the NV with all of the ¹³C. A crossover must be avoided, and this can be realized using advanced decoupling techniques.⁷⁰ The

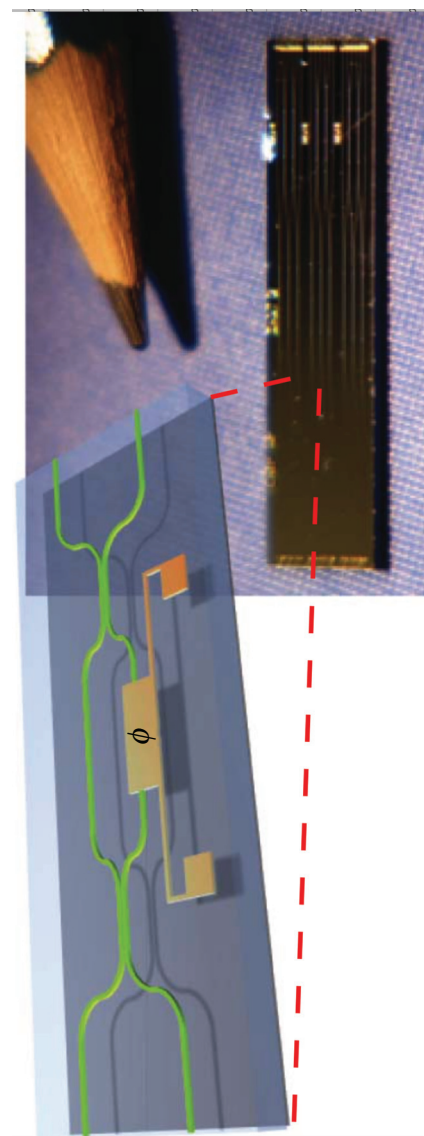


FIG. 10. (a) Quantum computing with photons. An interferometer with controlled phase shift for single-qubit operations and multi-photon entangled state manipulation. Reproduced with permission from T. D. Ladd *et al.*, “Quantum computers,” *Nature* **464**(7285), 45–53 (2010).⁹⁸

most effective way to achieve this is to directly link the gate with the decoupling sequence. Because the ¹³C have different positions with respect to the NV center, each hyperfine coupling is different. If the NV is in the state $m = 1$ or $m = -1$, the hyperfine interaction leads to a shift in the RF frequency, which is in resonance with the spin of ¹³C. It is therefore possible to address different ¹³C spins separately. The decoherence of the NV is first used to check its environment—to determine how many ¹³C spins are situated close by as well as the strengths with which they are interacting—by sweeping the RF frequency. Figure 13 shows the NV decoherence as a function of the RF frequency. The different frequencies are

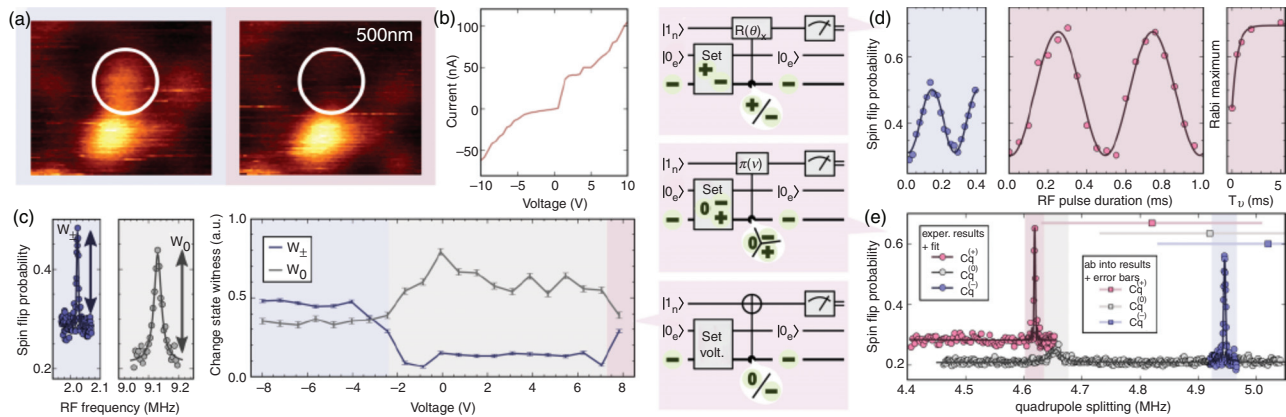


FIG. 11. (a) Confocal microscopy image of single NV centers. The left image (light-blue background) was recorded at a voltage corresponding to the NV charge state. In the right image (light-red background), the NV's fluorescence is quenched by reversing the gate voltage. The blue, gray, and pink colors denote NV^- , NV^0 , and NV^+ , respectively, throughout the figure. (b) I – V characteristics of the surface gate structure. (c) The two spectra on the left show one of the ^{15}N nuclear spin transitions for the NV^\pm and NV^0 charge states. Their normalized amplitudes yield the charge state probabilities W^\pm and W^0 , respectively. W^\pm increases for any charge state exhibiting an electron spin state $m = 0$, as is expected for NV^+ ($S = 0, m = 0$). The graph on the right shows the charge state probabilities for varying voltages (error bars represent projection noise). The reappearance of the W^\pm signal at high voltages suggests the presence of NV^+ . (d) ^{15}N nuclear spins with Rabi oscillations between spin state $m_l = \pm 1/2$ for the NV^- ($m = 0$) and the tentative NV^+ charge state. The right curve shows the maxima of the NV^+ Rabi oscillation for varying durations of the initial NV^+ voltage application. We deduced an NV^+ settling time of 0.54 ± 0.08 ms. For the NV^- charge state, hyperfine interaction increases the Rabi frequency. (e) ^{14}N quadrupole splittings for the three known charge states (resonances of experimental spectra represented by circles, those of the theory by squares). Any magnetic hyperfine and nuclear Zeeman terms are subtracted. Reproduced with permission from M. Pfender *et al.*, "Protecting a diamond quantum memory by charge state control," *Nano Lett.* **17**(10), 5931–5937 (2017).⁵⁸

then used for the individual control of the NV. The method has many advantages. On the one hand, it is not necessary to use isotopically pure ^{12}C samples, or to implant or place the ^{13}C in the vicinity of the NV center. Diamond samples with a natural abundance of ^{13}C (1.1%) can simply be used. On the other hand, because the T_2 times of the nuclei at low temperatures are of the order of several minutes to hours, the state of the NV centers can be reset. Furthermore, in Ref. 100 a single NV center was coupled with up to 28 ^{13}C . This drastically increases the possibility of

scalability as only a few coupled NVs are needed to control a large number of qubits.

J. Mechanical control of NV-NV using AFM tips

In this proposal, the coupling is achieved via an AFM tip in which an NV center is located. The tip is moved over a surface with NV centers. The advantage is that the distance between the NV centers can be very large. The disadvantage of this method is that it takes a

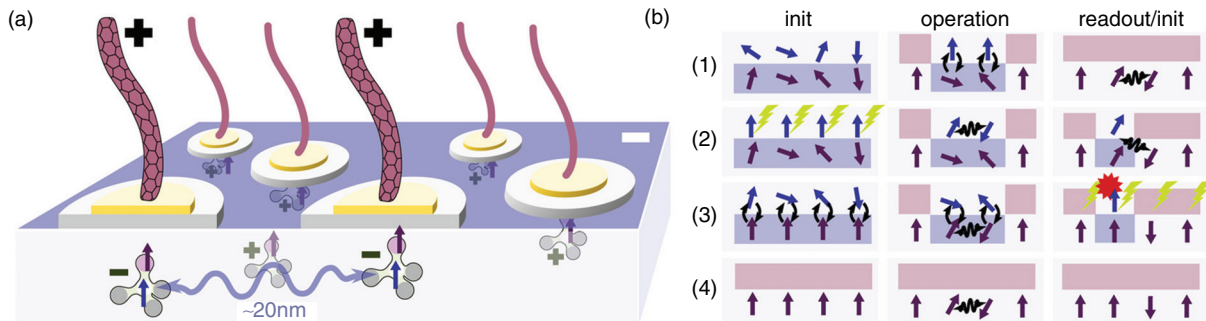


FIG. 12. (a) Schematic of individual NV nodes addressable via nanoscopic gate electrodes (gray, insulator; gold, electrode; purple, leads). NV centers under H-terminated surface are in the NV^+ state, and, therefore, do not couple with other nodes because of the lack of an electron spin, their nuclear spin state remains undisturbed, and they do not contribute to fluorescence response when illuminated. Individual electrodes with a positive voltage deplete the hole-conducting layer locally and shift the Fermi level to the stable NV^- region. Therefore, such NV centers can be coupled with their NV^- neighbors via magnetic dipole interaction and are optically accessible. Unsuitable NV nodes are not supplied with an electrode, and remain in NV^+ . (b) Sketch of modes of operation of the quantum register, with the charge states highlighted by the red and blue boxes, nuclear and electron spins represented by purple and blue arrows, respectively, laser represented in green, and fluorescence by red stars. Initialization: (1 – 2) Laser initializes all electron spins, (3) swaps to nuclear spins, and (4) switches to NV^+ for storage. Operation: (1) Swap two nuclear spins with electron spins in NV^- , (2) entangle the electron spins, (3) swap back to the nuclei, and (4) switch all NV centers to NV^+ . Readout/init: (1) Switch one NV to NV^- with an initialized electron spin, (2) correlate the electron spin with nuclear spin, (3) read out one electron spin and project the nuclear spins (2 – 3), single-shot readout, and (4) switch back to NV^+ . Reproduced with permission from M. Pfender *et al.*, "Protecting a diamond quantum memory by charge state control," *Nano Lett.* **17**(10), 5931–5937 (2017).⁵⁸

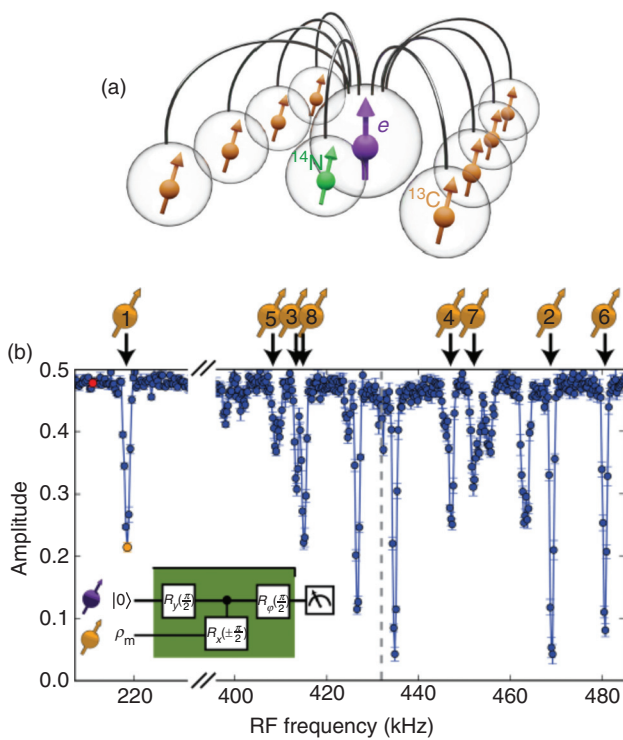


FIG. 13. (a) The electron spin of a single NV center in diamond acts as a central qubit and is connected by two-qubit gates to the intrinsic ¹⁴N nuclear spin and a further eight ¹³C nuclear spins surrounding the NV center. (b) Nuclear spin spectroscopy. After preparing the electron in a superposition state, the gate is applied at different RF frequencies ω . The electron spin is then measured along a basis in the equatorial plane defined by angle φ (see inset). Each data point corresponds to the fitted amplitude A of the function, where φ is swept from 0 to 360 deg., and φ_0 accounts for deterministic phase shifts induced on the electron by the RF field. By fitting the amplitude, we distinguish such deterministic phase shifts from a loss of coherence due to entangling interactions. The signals due to interactions with the eight ¹³C spins used in this work are labeled. The dashed gray line indicates the ¹³C Larmor frequency ω_L . Reproduced with permission from C. E. Bradley *et al.*, “A ten-qubit solid-state spin register with quantum memory up to one minute,” Phys. Rev. X 9(3), 031045 (2019), licensed under a Creative Commons Attribution (CC BY) license.⁷⁵

long time and can only be realized at low temperatures. Disturbances close to the surface also have to be overcome.¹⁰¹

K. Electron bus system: NV-P1-e-P1-NV

Manson *et al.*⁷³ recently proposed using an electron bus system involving substitutional nitrogen (P1 center). This is an adaptation of the method patented by Schenkel *et al.* for ³²P in silicon.¹⁰² The idea is based on the transfer of the NV spin state on a free electron that, used as a flying qubit, enables coupling with a large number of NV centers. Because the electrons can be controlled by electric fields, this method is flexible, and represents a direct link to conventional information technology. However, a direct ionization of the NV centers is challenging because the spin state of a single electron is not defined in the state $m = 0$ and is instead defined by a combination of one electron up and one down. In the state $m = \pm 1$, both electrons are in the same state

but photoionization is difficult. This problem can be solved if the spin state is transferred to a P1 center that is then ionized. However, the re-ionization (NV^0 to NV^-) to a defined spin state with a given electron is not easy. Preliminary experiments have thus far been unsuccessful.¹⁰³

L. Hybrid concepts: NV-superconducting qubits

In this approach, the NV centers are employed as storage elements for superconducting qubits. Because both systems operate at the same microwave frequency, the spin state can be exchanged between systems. An attempt was made to use an NV spin bath. The idea is to combine the functionality of superconducting qubits with a long T_2 time of NV centers. Due to the difficulty of coupling, the relevant experiments have so far been unsuccessful.^{104,105}

IV. FROM CLASSICAL QUANTUM INTERFACE TO QUANTUM DEVICES: READOUT OF QUBITS

As described in Sec. III, the readout (measurement) is one of the most important criteria for building a quantum computer. Technically, this can be done with the help of optical methods (i.e., the photon) or in electronic form (with electrons). With photons as well as electrons, the quantum state is determined several times without changing the state of the respective qubit or other qubits. This procedure is called the single-shot readout and is illustrated in Fig. 14.

A. Optical spin readout

The optical readout must be distinguished between those at low temperatures and at room temperature. The aim of the single-shot readout is to determine the spin state without changing the states of the neighboring NV centers. At room temperature, the direct spin state readout within a single shot cannot be achieved. The solution consists in transferring the spin state to an adjacent nuclear spin and then to measure it (through a CNOT gate). If the measurement is performed at the electron spin sublevel $m = 0$, the spin state of the nucleus is preserved and the measurement can be repeated several times.²⁶ At low temperatures, the situation is more favorable owing to the narrow linewidths. In such a case, a direct readout can be performed because the excitation of state $m = 0$ is achieved only at a certain frequency. This can now be repeated several times: If fluorescence occurs, the $m = 0$ state is confirmed; if it does not occur, it is the $m = \pm 1$ state. In principle, the problem of addressing emerges with optical readouts. With the optical setups generally used, the resolution is limited to approximately 250–400 nm ($\sim \lambda/2 \text{NA}$). However, the distance between the coupled NVs must not exceed 100 nm. A readout of individual NVs is therefore not possible. Attempts to eliminate the addressing by means of stimulated emission depletion (STED) microscopy¹⁰⁰ have been unsuccessful: The laser power of the depletion beam that is necessary to achieve the required resolution is too high and disturbs the coherence times of the nuclear spin.

B. Electrical spin readout

Photoelectrons can be used to readout the NV. The so-called photocurrent detection of magnetic resonance (PDMR) method has been known for a long time,^{106,107} but recently it has become possible to readout the spin state of single NV centers. This involves a two-photon process to ionize the NV center, and the laser power needs to

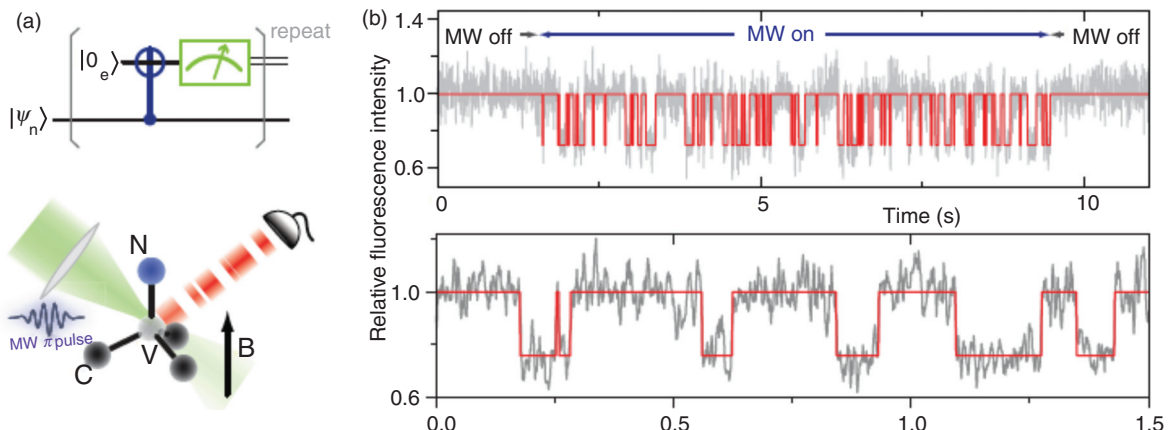


FIG. 14. (a) Single-shot readout reveals quantum jumps of a single nuclear spin in real time. (a) Representation of the single-shot readout scheme. (b) Normalized fluorescence time traces (gray) showing quantum jumps of a single nuclear spin in real time. When the microwave pulses (CNOT gates) are on, a telegraph-like signal appears, revealing the projective nature of this measurement. A low fluorescence intensity represents nuclear spin state -1_n and a high intensity indicates the state $0_n\rangle$ or $+1_n\rangle$. When the microwave pulses are off (upper trace), the fluorescent intensity remains high because it is not correlated with the nuclear spin state. Each data point was acquired by continuously repeating the readout scheme for 5 ms (2000 repetitions). Reproduced with permission from P. Neumann *et al.*, “Single-shot readout of a single nuclear spin,” *Science* **329**(5991), 542–544 (2010).

be chosen accordingly. The principle is described in Fig. 15. It has been shown that the use of a second laser beam speeds up NV recharging from NV^0 to NV^- . If this process is repeated several times, the number of photoelectrons comes to depend on the spin state of the NV center and can be determined accordingly. As with optical readout, a single shot can be performed at room temperature via a nuclear spin. At low temperature, a direct readout is also possible with PDMR. Addressing is carried out by placing an electrical contact over each NV center to which a suction voltage can be applied. Only NVs with the

correspondingly high suction voltages are thus read out. The readout lines can, for example, be attached as a gauze and switched accordingly. Thus it should be possible to read out 100 NV centers with only 20 lines, one row being read out at a time. It is also important to preserve the spin state as long as possible; otherwise, the arithmetic operation has to be repeated a larger number of times. However, even in such a case, the computational effort increases only linearly in time.

V. TECHNICAL REQUIREMENTS AND FABRICATION METHODS FOR SCALABLE DESIGN

A. Diamond in CMOS technology

The production of quantum computers at an industrial process can be achieved only if the structures of CMOS technology are transferred to processes necessary for the machining of diamond. Therefore, the necessary manufacturing processes, such as single-ion implantation and growth, need to be standardized. Comprehensive quality control, especially of the grown diamonds, must be defined and applied. We currently have a technological standard for diamond that is comparable to those in the 1960s and 1970s for silicon technology. Only in the 1980s, when it became possible to manufacture silicon of the same quality in a controlled manner, did the semiconductor industry develop at a large scale. The main techniques for the production of diamond qubits are chemical vapor deposition (CVD) growth, single-ion implantation, and thermal annealing. Other processes correspond to the current CMOS standard and can be transferred over directly.

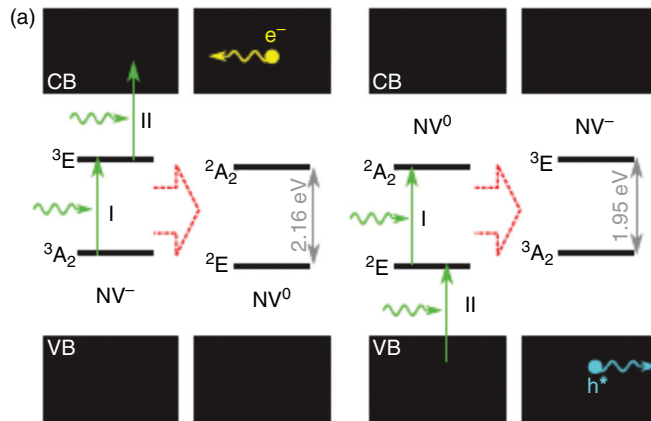


FIG. 15. Schematic representation of the experiment. (a) Simplified representation of charge carrier generation within one cycle of NV^- ionization and recovery. First, two photons produce a free electron in the conduction band (CB) and leave defects in the neutral charge state. Second, the two photons convert the neutral charge state back to NV^- while a free hole persists in the valence band (VB). I and II indicate the first and second transitions of the electrons, respectively, and e and h represent the electron and the hole, respectively. Reproduced with permission from P. Siyushev *et al.*, “Photoelectrical imaging and coherent spin-state readout of single nitrogen-vacancy centers in diamond,” *Science* **363**(6428), 728 (2019).

B. Growth techniques

The growth of suitable diamond layers represents a major hurdle in the production chain.¹⁰ Thus far, no standard CVD diamond is really available. Although the E6 company has made an initial subdivision with the introduction of optical, electronic, and quantum grades as well as set values for nitrogen content, other important parameters, such as hydrogen content, defects, and stress, have not been

standardized. There are especially large differences in hydrogen content. This is a problem that is hindering the industrialization of diamond products. This is a well-known chicken-and-egg problem. Because no suitably reproducible diamond layer is available, no standardized product can be developed, yet.

C. Deterministic creation of single NV centers with high resolution

The diffusion of atoms of almost all elements into diamond is negligibly small.¹⁷ This has the significant advantage that, once introduced, the structures are very stable in time and do not change even during subsequent healing.¹⁷ However, only ion implantation is suitable as a method for the production of dopants. Ion implantation techniques have been significantly improved in recent years, and procedures that allow for a mask-free deterministic implantation of single ions down to a few nanometers are now available [Fig. 16(a)].

It is therefore particularly advantageous to choose a diamond as pure as possible (with the lowest level of impurity atoms and crystalline defects) to implant individual ions and convert them into color centers by heat treatment. Although foreign atoms, such as nitrogen, can be introduced to diamond during growth and later converted into color centers by generating additional vacancies (e.g., by laser writing), the unconverted atoms (e.g., N atoms) interfere and lead to shorter coherence times. Likewise, it is not possible to create NVs with this method with a precision of a few nanometers, contrary to the case of ion implantation. The generation of color centers by ion implantation also has some disadvantages, however. For example, the ions lose their energy during penetration into the diamond by collisions not only with the electrons but also with the nuclei of the crystal atoms. This leads to larger deviations from the initial trajectory and the creation of defects. The resulting deviation from the desired path is called straggling. It is a well-known phenomenon, and high-resolution precision can be ensured by adapting the implantation energy to limit the straggling to a few nanometers or less. We recently achieved an N-to-NV conversion rate of up to 75% for 40 nm deep NVs. Whether the yield can be further improved, and whether the NV depth can be reduced to 10–20 nm are questions for actual research. The key was to dope the diamond with donors, and sulfur gave promising results.⁴⁷ The spin coherence time was extended by more than three times (with

respect to intrinsic diamond), and the charge stability of the NV color centers was increased. A conversion rate of almost 100% seems to be achievable by further optimization. An enhanced creation yield was also confirmed for other color centers. The significant advantage of color centers over alternative methods in a solid is that these centers consist of only two components, and thus always exhibit the same properties as long as the environment does not change. Because they are surrounded by the crystal lattice, in contrast to, e.g., quantum dots, a very high stability in terms of charge and temperature can be ensured.

In addition to the high conversion rate, a deterministic implantation of countable atoms with a high lateral resolution is necessary to create exactly one NV deterministically.¹⁰⁸ This problem has been solved by using different approaches: In the post-detection method, the implanted ions are detected after implantation by using secondary electrons or electron-hole pairs.^{109,110} In the pre-detection method, the implanted ion is detected before implantation using single ion sources^{111–113} or measuring the mirror charge.¹¹⁴ Pre-detection methods have the advantage that they help avoid false-negative implantation events.¹¹⁵ Thus, it may be the case that no ion is implanted (false positive), but never that two or more atoms are implanted. An optical inspection and subsequent repetition of the implantation procedure allow for the implantation of the missing atom. Figures 16 and 17 show sketches of single-ion implantation setups.

D. Thermal treatment

Now that the deterministic implantation of single ions at a high spatial resolution have been demonstrated, full scalability relies on the conversion of each implanted atom into an active qubit with the suitable properties. In the case of NV centers, N-to-NV conversion is achieved by thermal treatment that enables the diffusion of vacancies toward the implanted nitrogen and heals other implantation-induced defects. A wide range of temperatures, between 700 °C and 1200 °C for several hours, has been used to create NVs depending on the application. The excellent thermal stability of NV centers surpasses any other concurrent qubit. NV centers start to dissociate at about 1300 °C. The re-orientation of the NV, which would be an issue for qubit addressing, does not occur below 1000 °C.^{17,116} The diffusion of neutral vacancies has been determined experimentally to be about 1.5 nm²/s at 1000 °C with an activation energy of 2.12 eV¹¹⁷ or 1.8 nm²/s at 850 °C.¹¹⁸

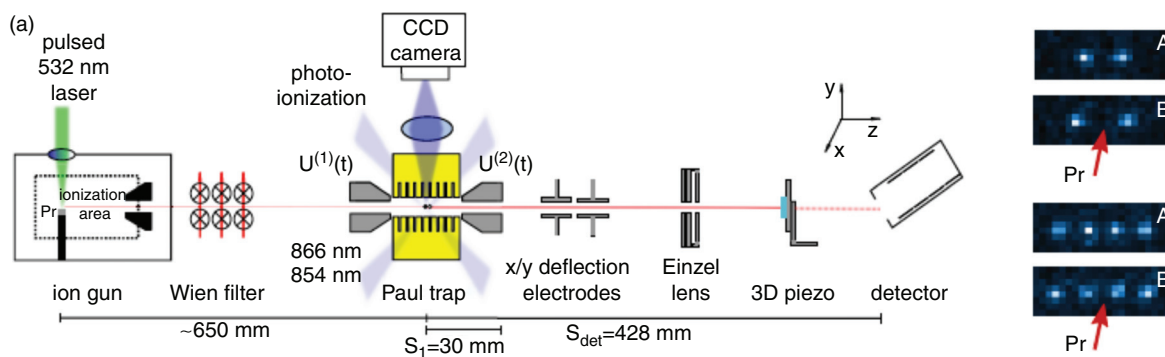


FIG. 16. (a) Sketch of single-ion implantation setup. (b) Fluorescence of the trapped ions imaged. (top) Pure Ca crystals; the distance between two Ca ions was 9.5 μm. (bottom) Crystals containing an additional Pr ion. Reproduced with permission from K. Groot-Berning *et al.*, “Deterministic single-ion implantation of rare-earth ions for nanometer-resolution color-center generation,” Phys. Rev. Lett. **123**(10), 106802 (2019).⁶⁴

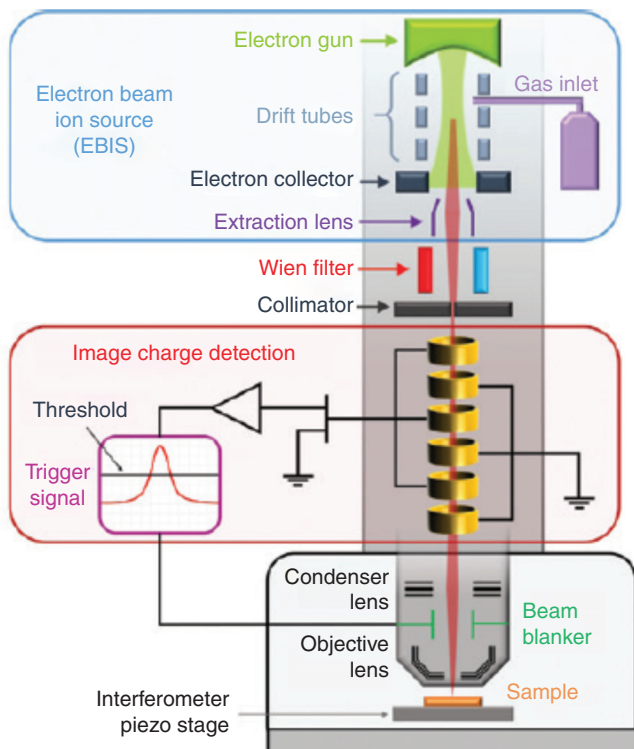


FIG. 17. Sketch of a deterministic single ion implanter based on mirror charge collection. Reproduced with permission from T. Herzog et al., “Creation of quantum centers in silicon using spatial selective ion implantation of high lateral resolution,” in 22nd International Conference on Ion Implantation Technology (IIT), Würzburg, Germany, 16–21 Sept. 2018 (IEEE, 2018), pp. 136–139.¹¹⁴

Nevertheless, a competing process to NV creation is the formation of V₂ or larger complexes, which easily form, during annealing as well as the implantation itself, especially for larger atoms.¹⁷ At an ion implantation energy suitable for 10–20-nm-deep qubits, the yield of NV creation is only a few percentage points.¹¹⁹ Each unconverted nitrogen, each divacancy, is a source of decoherence for the NVs.

Recent work at the single-center level has provided new insights into the birth, disappearance, and re-orientation of the NV with respect to the type of doping of diamond (see Sec. II C).^{46,47,116} This instance of charge-assisted defect engineering offers new possibilities for the targeted and enhanced formation of some color centers to the detriment of unwanted ones. Furthermore, the stability and spin properties of the NV[−] charge state are improved. In addition to NV centers, for which the creation was enhanced along an order of magnitude up to 75%, this method has also proved to work with SnV and MgV centers. Following the same idea of charging defects during thermal annealing to modify the formation and diffusion processes, it can also be tried to use light illumination or to apply a voltage to the sample. As well, rapid thermal annealing would add another degree of freedom. A recent method that uses femtosecond laser has also been shown to achieve local healing and induce NV centers from native nitrogen atoms.¹⁰⁸ Whether this method is also suitable for implanted nitrogen is the subject of ongoing research. Finally, the presence and quantity of hydrogen in high purity CVD-grown diamond needs to be

taken into account (and better studied) because hydrogen can easily diffuse and passivate the qubits.

VI. SUMMARIZING PERFORMANCE OF QUBITS BASED ON NV CENTERS

The current status of the NV-based qubits is shown in Table II. At present, 10 qubits can be fully controlled. In the relevant methods, the NV center is used to control the nuclear qubits consisting of ¹³C

TABLE II. Summary of the current performance status of NV-based qubits (based on input by T. H. Taminiau).

Quantum chips:	Value	Refs.	Remarks
Number of qubits demonstrated	7 qubits	75	Entangled GHz state
	10 qubits	75	Fully connected
	29 qubits	76	Rudimentary qubits controlled
Chip linked	2	120	Optical interconnection
Coherence			
T ₂ (e qubit)	2.4 ms 0.6 s 1.5 s	69 121 70	Temperature 300 K 77 K 4 K
T ₂ (n qubits)	2 s 1 min	9 75	300 K 4 K
Control gates			
Fidelity: single qubit gate	99.995%	78	300 K
Fidelity: two qubit (e-e)	>97%	122	300 K
Fidelity: (e-n)	99.2%	78	300 K
Speed: single qubit gate (e)	<10 ns	38	300 K
Speed: two qubit gate (e-n)	700 ns	78	300 K
Measurement			
Fidelity (e)	98%	120	
Projectiveness	>99%	123	Post-measurement state
Measurement time	3 μs	120	
Fidelity three-qubit parity measurement	0.63	123	
Initialization			
Fidelity	99.9%	124	Excitation of electron
Speed	200 ns	88	Excitation of electron
Chip to chip interconnection			
Entanglement fidelity	92%	120	
Distance	>1 km	120	
Sub routines			
Algorithm: Q-search	125	Temperature 300 K	
Algorithm: Q simulation	126	300 K	
Quantum error correction 3-qubit code	91	300 K	
Logical qubits	92	4 K	

atoms in its immediate vicinity (a maximum of two lattice sites away). This method can easily be enhanced by using entangled NV centers. The NV center has very good coherence times even at room temperature, which allows for the implementation of simple quantum algorithms that currently cannot be used in competing cryogenic systems. The fidelity obtained is comparable to that of a superconducting qubit system or even higher. The error correction as well as the first quantum algorithm have already been verified.

VII. CONCLUSIONS AND OUTLOOK

In recent years, a large number of proposals have been made for a quantum computer based on color centers in diamond. However, many of them do not go beyond the idea of such a device. Recently, however, techniques and procedures such as deterministic single-ion implantation have been developed, which, after special treatment of the diamond, can produce NV centers with high yields. Solutions have also been found to electrically read out single NV centers by means of the photocurrent. It has been shown that an NV with many ^{13}C nuclei can be interlaced. These findings may represent a game-changer, even if the coupling to the ^{13}C nuclei is possible only at low temperature (otherwise, the addressing of separate ^{13}C nuclear spins is hindered by the broadening of the microwave resonances).

The next steps in future research in this area should involve building a system using the magnetic dipole-dipole coupling of a 30-nm pitch grating of NVs, where each NV center is connected to several (e.g., ten) ^{13}C qubits. The depth of the NV centers should be in the range of 10 to 20 nm so that their electrical readouts and control by microwave pulses can be implemented by crossed nanowires above each NV. The use of crossed wires enables the generation of circularly polarized microwave pulses and allows for the addressing of individual NV centers. Such a scheme cannot only enable the coupling of 100 NV qubits within a 10×10 grid controlled with 20 nanowires, but can provide a one-kilo qubit system (because each NV can further control up to ten ^{13}C qubits). The scheme can be modified if the coupling is carried out using photons, free electrons, phonons, and so on. Furthermore, this concept allows for the stabilization of the NV qubits by the ^{13}C spin bath and operation at room temperature.

In Europe, a consortium with several large companies has already been formed to investigate this new scheme. But even if many detailed questions are still open, the relevant technical and technological challenges are pushing prevalent technology to new borders that may also open new avenues for applications in other fields. The current race to produce the first fully functional quantum computer is comparable to the race to put the first human on the moon and can similarly inspire people.

AUTHOR CONTRIBUTIONS

All authors contributed equally to this work.

ACKNOWLEDGMENTS

The authors acknowledge the funding from the European Union's Horizon 2020 research and innovation program under grant agreement No. 820394 (ASTERIQS), from the European Union project MICROSENS (No. BMBF 16KIS0831) and from the Bundesministerium für Bildung und Forschung (project DiaQuantFab). The authors acknowledge the support from Leipzig University for Open Access Publishing. We thank Professor T. H. Taminiau (Uni. Delft) for providing the content for Table II.

DATA AVAILABILITY

Data sharing is not applicable to this article as no new data were created or analyzed in this study.

REFERENCES

- ¹A. Gruber *et al.*, "Magnetic-resonance on single molecules in an external magnetic-field: The Zeeman-Effect of a single-electron spin and determination of the orientation of individual molecules," *Chem. Phys. Lett.* **242**(4–5), 465–470 (1995).
- ²J. Wrachtrup, S. Y. Kilin, and A. P. Nizovtsev, "Quantum computation using the C-13 nuclear spins near the single NV defect center in diamond," *Opt. Spectrosc.* **91**(3), 429–437 (2001).
- ³P. Hemmer and J. Wrachtrup, "Where is my quantum computer?" *Science* **324**(5926), 473–474 (2009).
- ⁴J. R. Weber *et al.*, "Quantum computing with defects," *Proc. Nat. Acad. Sci. USA* **107**(19), 8513–8518 (2010).
- ⁵L. Childress *et al.*, "Coherent dynamics of coupled electron and nuclear spin qubits in diamond," *Science* **314**(5797), 281–285 (2006).
- ⁶F. Jelezko and J. Wrachtrup, "Read-out of single spins by optical spectroscopy," *J. Phys.-Condens. Matter* **16**(30), R1089–R1104 (2004).
- ⁷F. Jelezko *et al.*, "Observation of coherent oscillations in a single electron spin," *Phys. Rev. Lett.* **92**(7), 076401 (2004).
- ⁸F. Jelezko *et al.*, "Observation of coherent oscillation of a single nuclear spin and realization of a two-qubit conditional quantum gate," *Phys. Rev. Lett.* **93**(13), 130501 (2004).
- ⁹P. C. Maurer *et al.*, "Room-temperature quantum bit memory exceeding one second," *Science* **336**(6086), 1283–1286 (2012).
- ¹⁰G. Balasubramanian *et al.*, "Ultralong spin coherence time in isotopically engineered diamond," *Nat. Mater.* **8**(5), 383–387 (2009).
- ¹¹P. Zoller *et al.*, "Quantum information processing and communication," *Eur. Phys. J. D* **36**(2), 203–228 (2005).
- ¹²P. Neumann *et al.*, "Quantum register based on coupled electron spins in a room-temperature solid," *Nat. Phys.* **6**(4), 249–253 (2010).
- ¹³S. Yang *et al.*, "High-fidelity transfer and storage of photon states in a single nuclear spin," *Nat. Photonics* **10**(8), 507 (2016).
- ¹⁴T. Staudacher *et al.*, "Nuclear magnetic resonance spectroscopy on a (5-nanometer)³ sample volume," *Science* **339**(6119), 561–563 (2013).
- ¹⁵S. Schmitt *et al.*, "Submillihertz magnetic spectroscopy performed with a nanoscale quantum sensor," *Science* **356**(6340), 832–836 (2017).
- ¹⁶I. Schwartz *et al.*, "Blueprint for nanoscale NMR," *Sci. Rep.* **9**, 6938 (2019).
- ¹⁷T. Lühmann *et al.*, "Screening and engineering of colour centres in diamond," *J. Phys. D-Appl. Phys.* **51**(48), 483002 (2018).
- ¹⁸T. H. Taminiau, "Quantum information and networks with spins in diamond," in *Proceedings of 2014 Conference on Lasers and Electro-Optics*, San Jose, California (June 8–13, 2014).
- ¹⁹F. Jelezko, "Diamond based quantum technologies," *EPJ Web of Conferences* **190**, 01003 (2018).
- ²⁰H. Kaufmann *et al.*, "Scalable creation of long-lived multipartite entanglement," *Phys. Rev. Lett.* **119**(15), 150503 (2017).
- ²¹H. Kaufmann *et al.*, "Fast ion swapping for quantum-information processing," *Phys. Rev. A* **95**(5), 052319 (2017).
- ²²F. Arute *et al.*, "Quantum supremacy using a programmable superconducting processor," *Nature* **574**(7779), 505 (2019).
- ²³M. Veldhorst *et al.*, "Silicon CMOS architecture for a spin-based quantum computer," *Nat. Communications* **8**, 1766 (2017).
- ²⁴T. Teraji, "Isotopic enrichment of diamond using microwave plasma-assisted chemical vapor deposition with high carbon conversion efficiency," *Thin Solid Films* **557**, 231–236 (2014).
- ²⁵M. W. Doherty *et al.*, "Theory of the ground-state spin of the NV⁻ center in diamond," *Phys. Rev. B* **85**(20), 205023 (2012).
- ²⁶P. Neumann *et al.*, "Single-shot readout of a single nuclear spin," *Science* **329**(5991), 542–544 (2010).
- ²⁷R. John *et al.*, "Bright optical centre in diamond with narrow, highly polarised and nearly phonon-free fluorescence at room temperature," *New J. Phys.* **19**, 053008 (2017).

- ²⁸S. Y. Lee *et al.*, "Readout and control of a single nuclear spin with a metastable electron spin ancilla," *Nat. Nanotechnol.* **8**(7), 487–492 (2013).
- ²⁹D. D. Sukachev *et al.*, "Silicon-vacancy spin qubit in diamond: A quantum memory exceeding 10 ms with single-shot state readout," *Phys. Rev. Lett.* **119**(22), 223602 (2017).
- ³⁰M. W. Doherty *et al.*, "The nitrogen-vacancy colour centre in diamond," *Phys. Rep.* **528**(1), 1–45 (2013).
- ³¹B. K. Ofori-Okai *et al.*, "Spin properties of very shallow nitrogen vacancy defects in diamond," *Phys. Rev. B* **86**(8), 081406 (2012).
- ³²J. Wrachtrup and F. Jelezko, "Processing quantum information in diamond," *J. Phys.-Condens. Matter* **18**(21), S807–S824 (2006).
- ³³P. Balasubramanian *et al.*, "Discovery of ST1 centers in natural diamond," *Nanophotonics* **8**(11), 1993–2002 (2019).
- ³⁴D. A. Broadway *et al.*, "Quantum probe hyperpolarisation of molecular nuclear spins," *Nat. Communications* **9**, 1246 (2018).
- ³⁵L. Rondin *et al.*, "Magnetometry with nitrogen-vacancy defects in diamond," *Rep. Prog. Phys.* **77**(5), 056503 (2014).
- ³⁶J. P. Tetienne *et al.*, "Magnetic-field-dependent photodynamics of single NV defects in diamond: An application to qualitative all-optical magnetic imaging," *New J. Phys.* **14**, 103033 (2012).
- ³⁷G. D. Fuchs *et al.*, "Excited-state spin coherence of a single nitrogen-vacancy centre in diamond," *Nat. Phys.* **6**(9), 668–672 (2010).
- ³⁸G. D. Fuchs *et al.*, "Gigahertz dynamics of a strongly driven single quantum spin," *Science* **326**(5959), 1520–1522 (2009).
- ³⁹J. Tisler *et al.*, "Highly efficient FRET from a single nitrogen-vacancy center in nanodiamonds to a single organic molecule," *ACS Nano* **5**(10), 7893–7898 (2011).
- ⁴⁰P. Tamarat *et al.*, "Spin-flip and spin-conserving optical transitions of the nitrogen-vacancy centre in diamond," *New J. Phys.* **10**, 045004 (2008).
- ⁴¹F. Dolde *et al.*, "High-fidelity spin entanglement using optimal control," *Nat. Communications* **5**, 3371 (2014).
- ⁴²F. Dolde *et al.*, "Room-temperature entanglement between single defect spins in diamond," *Nat. Phys.* **9**(3), 139–143 (2013).
- ⁴³Y. Chou, S. Y. Huang, and H. S. Goan, "Optimal control of fast and high-fidelity quantum gates with electron and nuclear spins of a nitrogen-vacancy center in diamond," *Phys. Rev. A* **91**(5), 052315 (2015).
- ⁴⁴Y. Chu *et al.*, "All-optical control of a single electron spin in diamond," *Phys. Rev. A* **91**(2), 021801 (2015).
- ⁴⁵T. Yamamoto *et al.*, "Extending spin coherence times of diamond qubits by high-temperature annealing," *Phys. Rev. B* **88**(7), 075206 (2013).
- ⁴⁶F. F. de Oliveira *et al.*, "Tailoring spin defects in diamond by lattice charging," *Nat. Communications* **8**, 15409 (2017).
- ⁴⁷T. Lüthmann *et al.*, "Coulomb-driven single defect engineering for scalable qubits and spin sensors in diamond," *Nat. Communications* **10**, 4956 (2019).
- ⁴⁸T. Vogel, J. Meijer, and A. Zaitsev, "Highly effective p-type doping of diamond by MeV ion implantation of boron," *Diamond Related Mater.* **13**(10), 1822–1825 (2004).
- ⁴⁹E. Gheeraert *et al.*, "n-type doping of diamond by sulfur and phosphorus," *Diamond Related Mater.* **11**(3–6), 289–295 (2002).
- ⁵⁰Y. Yamazaki *et al.*, "Defect creation in diamond by hydrogen plasma treatment at room temperature," *Phys. B-Condens. Matter* **376–377**, 327–330 (2006).
- ⁵¹S. Salustro *et al.*, "Hydrogen atoms in the diamond vacancy defect: A quantum mechanical vibrational analysis," *Carbon* **129**, 349–356 (2018).
- ⁵²S. H. Connell *et al.*, "Hydrogen and hydrogen-like defects in diamond," *Mater. Sci. Forum* **258–263**, 751–756 (1997).
- ⁵³J. C. Arnault *et al.*, "Enhanced deuterium diffusion in boron doped monocrystalline diamond films using bias-assisted MPCVD," *Phys. Lett. A* **374**(31–32), 3254–3257 (2010).
- ⁵⁴J. Barjon *et al.*, "Hydrogen-induced passivation of boron acceptors in monocrystalline and polycrystalline diamond," *Phys. Chem. Chem. Phys.* **13**(24), 11511–11516 (2011).
- ⁵⁵N. B. Manson *et al.*, "NV–N⁺ pair centre in 1b diamond," *New J. Phys.* **20**, 113037 (2018).
- ⁵⁶T. Mittiga *et al.*, "Imaging the local charge environment of nitrogen-vacancy centers in diamond," *Phys. Rev. Lett.* **121**(24), 246402 (2018).
- ⁵⁷C. Schreyvogel *et al.*, "Active and fast charge-state switching of single NV centres in diamond by in-plane Al-Schottky junctions," *Beilstein J. Nanotechnol.* **7**, 1727–1735 (2016).
- ⁵⁸M. Pfender *et al.*, "Protecting a diamond quantum memory by charge state control," *Nano Lett.* **17**(10), 5931–5937 (2017).
- ⁵⁹C. Schreyvogel *et al.*, "Tuned NV emission by in-plane Al-Schottky junctions on hydrogen terminated diamond," *Sci. Rep.* **4**, 3634 (2015).
- ⁶⁰M. V. Hauf *et al.*, "Addressing single nitrogen-vacancy centers in diamond with transparent in-plane gate structures," *Nano Lett.* **14**(5), 2359–2364 (2014).
- ⁶¹D. P. DiVincenzo, "The physical implementation of quantum computation," *Fortschritte Der Phys.-Prog. Phys.* **48**(9–11), 771–783 (2000).
- ⁶²A. Barenco *et al.*, "Elementary gates for quantum computation," *Phys. Rev. A* **52**(5), 3457–3467 (1995).
- ⁶³D. P. DiVincenzo, "Quantum computation," *Science* **270**(5234), 255–261 (1995).
- ⁶⁴K. Groot-Berning *et al.*, "Deterministic single-ion implantation of rare-earth ions for nanometer-resolution color-center generation," *Phys. Rev. Lett.* **123**(10), 106802 (2019).
- ⁶⁵J. Harrison, M. J. Sellars, and N. B. Manson, "Optical spin polarisation of the N–V centre in diamond," *J. Luminescence* **107**(1–4), 245–248 (2004).
- ⁶⁶J. Harrison, M. J. Sellars, and N. B. Manson, "Measurement of the optically induced spin polarisation of N–V centre in diamond," *Diamond Related Mater.* **15**(4–8), 586–588 (2006).
- ⁶⁷A. P. Nizovtsev *et al.*, "Non-flipping ¹³C spins near an NV center in diamond: Hyperfine and spatial characteristics by density functional theory simulation of the C₅₁₀[NV]H₂₅₂ cluster," *New J. Phys.* **20**, 023022 (2018).
- ⁶⁸H. Morishita *et al.*, "Extension of the coherence time by generating MW dressed states in a single NV in diamond," *Sci. Rep.* **9**, 13318 (2019).
- ⁶⁹E. D. Herbschleb *et al.*, "Ultra-long coherence times amongst room-temperature solid-state spins," *Nat. Communications* **10**, 3766 (2019).
- ⁷⁰M. H. Abobeih *et al.*, "One-second coherence for a single electron spin coupled to a multi-qubit nuclear-spin environment," *Nat. Communications* **9**, 2552 (2018).
- ⁷¹H. Bernien *et al.*, "Heralded entanglement between solid-state qubits separated by three metres," *Nature* **497**(7447), 86–90 (2013).
- ⁷²T. Plakhotnik, M. W. Doherty, and N. B. Manson, "Electron-phonon processes of the nitrogen-vacancy center in diamond," *Phys. Rev. B* **92**(8), 081203 (2015).
- ⁷³L. M. Oberg *et al.*, "Spin coherent quantum transport of electrons between defects in diamond," *Nanophotonics* **8**(11), 1975–1984 (2019).
- ⁷⁴M. W. Doherty *et al.*, "Towards a room-temperature spin quantum bus in diamond via electron photoionization, transport, and capture," *Phys. Rev. X* **6**(4), 041035 (2016).
- ⁷⁵C. E. Bradley *et al.*, "A ten-qubit solid-state spin register with quantum memory up to one minute," *Phys. Rev. X* **9**(3), 031045 (2019).
- ⁷⁶M. H. Abobeih *et al.*, "Atomic-scale imaging of a 27-nuclear-spin cluster using a quantum sensor," *Nature* **576**(7787), 411 (2019).
- ⁷⁷D. D. Awschalom *et al.*, "Quantum technologies with optically interfaced solid-state spins," *Nat. Photonics* **12**(9), 516–527 (2018).
- ⁷⁸X. Rong *et al.*, "Experimental fault-tolerant universal quantum gates with solid-state spins under ambient conditions," *Nat. Communications* **6**, 8748 (2015).
- ⁷⁹Y. Wang *et al.*, "Quantum simulation of helium hydride cation in a solid-state spin register," *AC Nano* **9**(8), 7769–7774 (2015).
- ⁸⁰J. F. Haase *et al.*, "Soft quantum control for highly selective interactions among joint quantum systems," *Phys. Rev. Lett.* **121**(5), 050402 (2018).
- ⁸¹A. Sipahigil *et al.*, "An integrated diamond nanophotonics platform for quantum-optical networks," *Science* **354**(6314), 847–850 (2016).
- ⁸²J. T. Muhonen *et al.*, "Quantifying the quantum gate fidelity of single-atom spin qubits in silicon by randomized benchmarking," *J. Phys.-Condens. Matter* **27**(15), 154205 (2015).
- ⁸³J. T. Muhonen *et al.*, "Storing quantum information for 30 seconds in a nano-electronic device," *Nat. Nanotechnol.* **9**(12), 986–991 (2014).
- ⁸⁴M. Kjaergaard *et al.*, "Superconducting qubits: Current state of play," *Annu. Rev. Condens. Matter Phys.* **11**, 369–395 (2020).

- ⁸⁵R. Barends *et al.*, "Superconducting quantum circuits at the surface code threshold for fault tolerance," *Nature* **508**(7497), 500–503 (2014).
- ⁸⁶J. M. Nichol *et al.*, "High-fidelity entangling gate for double-quantum-dot spin qubits," *NPJ Quantum Inf.* **3**, 3 (2017).
- ⁸⁷W. Huang *et al.*, "Fidelity benchmarks for two-qubit gates in silicon," *Nature* **569**(7757), 532 (2019).
- ⁸⁸A. Reiserer *et al.*, "Robust quantum-network memory using decoherence-protected subspaces of nuclear spins," *Phys. Rev. X* **6**(2), 021040 (2016).
- ⁸⁹T. H. Taminiau *et al.*, "Universal control and error correction in multi-qubit spin registers in diamond," *Nat. Nanotechnol.* **9**(3), 171–176 (2014).
- ⁹⁰J. Cramer *et al.*, "Repeated quantum error correction on a continuously encoded qubit by real-time feedback," *Nat. Communications* **7**, 11526 (2016).
- ⁹¹G. Waldherr *et al.*, "Quantum error correction in a solid-state hybrid spin register," *Nature* **506**(7487), 204 (2014).
- ⁹²J. Casanova, Z. Y. Wang, and M. B. Plenio, "Noise-resilient quantum computing with a nitrogen-vacancy center and nuclear spins," *Phys. Rev. Lett.* **117**(13), 130502 (2016).
- ⁹³A. P. Nizovtsev *et al.*, "Quantum registers based on single NV + n C-13 centers in diamond: I. The spin Hamiltonian method," *Opt. Spectrosc.* **108**(2), 230–238 (2010).
- ⁹⁴J. H. Shim *et al.*, "Robust dynamical decoupling for arbitrary quantum states of a single NV center in diamond," *Epl* **99**(4), 40004 (2012).
- ⁹⁵P. Jamonneau *et al.*, "Competition between electric field and magnetic field noise in the decoherence of a single spin in diamond [93, 024305 (2016)]," *Phys. Rev. B* **99**(24), 249903 (2019).
- ⁹⁶R. Wunderlich *et al.*, "Optically induced cross relaxation via nitrogen-related defects for bulk diamond ¹³C hyperpolarization," *Phys. Rev. B* **96**(22), 220407 (2017).
- ⁹⁷N. Y. Yao *et al.*, "Scalable architecture for a room temperature solid-state quantum information processor," *Nat. Communications* **3**, 800 (2012).
- ⁹⁸T. Gaebel *et al.*, "Room-temperature coherent coupling of single spins in diamond," *Nat. Phys.* **2**(6), 408–413 (2006).
- ⁹⁹T. D. Ladd *et al.*, "Quantum computers," *Nature* **464**(7285), 45–53 (2010).
- ¹⁰⁰D. J. Klionsky *et al.*, "Guidelines for the use and interpretation of assays for monitoring autophagy (3rd edition)," *Autophagy* **12**(1), 1–222 (2016).
- ¹⁰¹S. Castelletto *et al.*, "Advances in diamond nanofabrication for ultrasensitive devices," *Microsystems Nanoengineering* **3**, 17061 (2017).
- ¹⁰²T. Schenkel *et al.*, "Deterministic doping and the exploration of spin qubits," *API Conf. Proc.* **1640**, 124 (2015).
- ¹⁰³M. S. J. Barson *et al.*, "The fine structure of the neutral nitrogen-vacancy center in diamond," *Nanophotonics* **8**(11), 1985–1991 (2019).
- ¹⁰⁴C. Grezes *et al.*, "Towards a spin-ensemble quantum memory for superconducting qubits," *C. R. Phys.* **17**(7), 693–704 (2016).
- ¹⁰⁵T. Douce *et al.*, "Coupling a single nitrogen-vacancy center to a superconducting flux qubit in the far-off-resonance regime," *Phys. Rev. A* **92**(5), 052335 (2015).
- ¹⁰⁶F. M. Hrubesch *et al.*, "Efficient electrical spin readout of NV - Centers in diamond," *Phys. Rev. Lett.* **118**(3), 037601 (2017).
- ¹⁰⁷P. Siyushev *et al.*, "Photoelectrical imaging and coherent spin-state readout of single nitrogen-vacancy centers in diamond," *Science* **363**(6428), 728 (2019).
- ¹⁰⁸J. M. Smith *et al.*, "Colour centre generation in diamond for quantum technologies," *Nanophotonics* **8**(11), 1889–1906 (2019).
- ¹⁰⁹T. Shinada *et al.*, "Opportunity of single atom control for quantum processing in silicon and diamond," in *Proceedings of 2014 IEEE Silicon Nanoelectronics Workshop (SNW)*, Honolulu, HI (2014), pp. 1–2.
- ¹¹⁰D. N. Jamieson *et al.*, "Deterministic doping," *Mater. Sci. Semicond. Process.* **62**, 23–30 (2017).
- ¹¹¹J. Meijer *et al.*, "Concept of deterministic single ion doping with sub-nm spatial resolution," *Appl. Phys. A* **83**(2), 321–327 (2006).
- ¹¹²J. Meijer *et al.*, "Towards the implanting of ions and positioning of nanoparticles with nm spatial resolution," *Appl. Phys. A* **91**(4), 567–571 (2008).
- ¹¹³W. Schnitzler *et al.*, "Deterministic ultracold ion source targeting the Heisenberg limit," *Phys. Rev. Lett.* **102**(7), 070501 (2009).
- ¹¹⁴T. Herzig *et al.*, "Creation of quantum centers in silicon using spatial selective ion implantation of high lateral resolution," in *22nd International Conference on Ion Implantation Technology (IIT)*, Würzburg, Germany, 16–21 Sept. 2018 (IEEE, 2018), pp. 136–139.
- ¹¹⁵P. Racke *et al.*, "Nanoscale ion implantation using focussed highly charged ions," *New J. Phys.* **22**(8), 083028 (2020).
- ¹¹⁶S. Chakravarthi *et al.*, "Window into NV center kinetics via repeated annealing and spatial tracking of thousands of individual NV centers," *Phys. Rev. Mater.* **4**(2), 023402 (2020).
- ¹¹⁷S. Onoda *et al.*, "Diffusion of vacancies created by high-energy heavy ion strike into diamond," *Phys. Status Solidi A* **214**(11), 1700160 (2017).
- ¹¹⁸S. T. Alsid *et al.*, "Photoluminescence decomposition analysis: A technique to characterize N-V creation in diamond," *Phys. Rev. Appl.* **12**(4), 044003 (2019).
- ¹¹⁹S. Pezzagna *et al.*, "Nanoscale engineering and optical addressing of single spins in diamond," *Small* **6**(19), 2117–2121 (2010).
- ¹²⁰B. Hensen *et al.*, "Loophole-free Bell inequality violation using electron spins separated by 1.3 kilometres," *Nature* **526**(7575), 682–686 (2015).
- ¹²¹N. Bar-Gill *et al.*, "Solid-state electronic spin coherence time approaching one second," *Nat. Communications* **4**, 1743 (2013).
- ¹²²T. Yamamoto *et al.*, "Strongly coupled diamond spin qubits by molecular nitrogen implantation," *Phys. Rev. B* **88**(20), 201201 (2013).
- ¹²³S. B. van Dam *et al.*, "Multipartite entanglement generation and contextuality tests using nondestructive three-qubit parity measurements," *Phys. Rev. Lett.* **123**(5), 050401 (2019).
- ¹²⁴N. Kalb *et al.*, "Dephasing mechanisms of diamond-based nuclear-spin memories for quantum networks," *Phys. Rev. A* **97**(6), 062330 (2018).
- ¹²⁵T. van der Sar *et al.*, "Decoherence-protected quantum gates for a hybrid solid-state spin register," *Nature* **484**(7392), 82–86 (2012).
- ¹²⁶Z.-Y. Wang *et al.*, "Delayed entanglement echo for individual control of a large number of nuclear spins," *Nat. Communications* **8**, 14660 (2017).